frontiers in Marine Science

TYPE Original Research
PUBLISHED 04 September 2026
DOI 10.3389/fmars.2026.1881744

OPEN ACCESS

EDITED BY
Kumbukani Mzengereza,
Mzuzu University, Malawi

REVIEWED BY
Qicheng Meng,
Ministry of Natural Resources, China
Jaynos R. Cortes,
Surigao del Sur State University,
Philippines

*CORRESPONDENCE
Chelsea Kimball
chelseakimball1@gmail.com

RECEIVED 14 May 2026
REVISED 14 June 2026
ACCEPTED 23 June 2026
PUBLISHED 04 September 2026

CITATION
Kimball C and Wosnik M (2026) Effects of wave-powered water pump upwelling on kelp mariculture: a case study for Gulf of Maine.
Front. Mar. Sci. 13:1881744.
doi: 10.3389/fmars.2026.1881744

Effects of wave-powered water pump upwelling on kelp mariculture: a case study for Gulf of Maine

Chelsea Kimball* and Martin Wosnik

Atlantic Marine Energy Center, University of New Hampshire, Durham, NH, United States

In kelp aquaculture, higher nitrate concentration increases productivity, and water temperatures within a favorable range promote kelp survival. In specific oceanic regions these environmental conditions can be produced by artificial upwelling. This work explores whether wave-powered artificial upwelling can modify local environmental conditions to enhance kelp mariculture productivity. A coupled physical-biogeochemical modeling feasibility study was developed using multi-year empirical oceanographic data of temperature, nitrate concentrations, and wave conditions at an ocean case study site in the Gulf of Maine. The study is limited in its approach where mixing conditions are assumed to be ideal, and horizontal advection is assumed to be negligible (or periodic within a much larger kelp farm). The model estimates that wave-powered upwelling can decrease the water temperature by an average of 1.0 ± 0.15 °C from June through October, and increase nitrate concentration by an average of 0.1–1.1 μmol L^{-1} from June through September depending on parameter uncertainties within a simplified model kelp farm. Additional analysis of farm-scale boundary conditions suggests that the spatial distribution and degree of mixing upwelled water strongly influences the extent of nitrate increase and cooling within kelp farms. The environmental changes in the example kelp farm due to wave-powered upwelling are then applied to a validated kelp growth model with empirical surface current magnitudes and irradiance data, producing an estimate of $0.9^{+1.1}_{-0.0}$ DMT ha^{-1} yr^{-1} (or approximately $9.5\%^{+1.6\%}_{-10\%}$) of additional kelp grown. The kelp growth model assumes that nitrate is the only limiting nutrient in kelp growth, and has some other limitations. This framework facilitates further investigation of wave-powered upwelling as a scalable ocean-based strategy for sustainable kelp aquaculture. Combined, these findings suggest that wave-powered artificial upwelling may enhance kelp productivity under nutrient-limited and seasonally warm conditions in temperate marine ecosystems.

KEYWORDS
aquaculture, artificial upwelling, kelp, mariculture, wave energy

1 Introduction

1.1 Motivation

Macroalgaes, such as kelp, are used globally in many industries, and typically have reduced atmospheric carbon emissions compared to other materials used for the same application (Farghali et al., 2023). One potential use for kelps is a feedstock for biofuels (V et al., 2021). A US Department of Energy project hypothesized that if large quantities of kelp can be grown at low cost, a renewable, nearly carbon-neutral fuel could potentially be sustainably sourced from US waters (Freeman and von Keitz, 2016). Kelp is also used in animal feeds, which may have the ability to decrease methane emissions from cattle, a significant contributor to anthropogenic greenhouse gas emissions (Molina-Alcaide et al., 2017; Min et al., 2021; Dhakal et al., 2024). Additionally, kelp farming does not require crop land, freshwater, or fertilizers, which reduces production costs and the use of valuable resources. By increasing yields of farmed kelp, at a reduced overall cost, there is a potential to supply a valuable feedstock to many industries with a lowered carbon footprint.

Kelps have been shown to experience increased growth when exposed to nutrient-rich and colder temperature water (Bolton and Luning, 1982). In some studies, with depth-cycling experiments, giant kelps were found to produce four times their biomass compared to control groups (Navarrete et al., 2021)[1]. Upwelling is a process that occurs naturally in the oceans due to wind, benthic topography, or sometimes instabilities due to variable density (Shan and Sheng, 2022). Natural upwelling is the cause of seasonal algal blooms and prevalence of increased fish stocks (Kirke, 2003), as it transports colder, nutrient-rich waters to the surface, which benefits many oceanic species. Upwelling can also be produced artificially by pumping water from greater depths to the surface. If this process could be powered by wave energy, it could further reduce costs and enhance the sustainability of growing kelp (Vershinskiy et al., 1987; White et al., 2010; Soloviev, 2016).

Since wave energy is abundantly available onsite in most kelp mariculture locations (Kilcher et al., 2021), it makes a logical power source for artificial upwelling. By utilizing a wave-powered water pump in a kelp mariculture operation, farmers could increase the amount of kelp grown within the same sea space, using natural processes, for relatively low additional cost. An ocean tested prototype and concept diagram for a wave-powered water pump installed within a kelp farm is shown in Figure 1.

1.2 Background

The global, annual macroalgae (i.e., seaweed) harvest was estimated at approximately 38 million wet metric tons in 2022, of which 97% was farmed (FAO, 2024). The majority of the kelp harvest originates in China, accounting for 60% of the global total (FAO, 2024) as seen in Table 1. China's main kelp crop species is *Saccharina japonica*, which is closely related to the main kelp crop species in the Gulf of Maine, *Saccharina latissima*, also referred to as sugar kelp (Zhang et al., 2022, Robidoux and Good, 2023). North America accounts for 1.4% of the global harvest, with the state of Maine in the United States being a major contributor. The United States had a farmed harvest of 979.1 wet metric tons in 2023, with 454 wet metric tons, almost half, from Maine (Robidoux and Good, 2023). The kelp industry in Maine has been experiencing significant growth rates in recent years with an average growth rate of 76% per annum between 2015 and 2024, outpacing the total global average growth rates of 5.8% per annum between 2000 and 2022 (FAO, 2024; Department of Maine Resources, 2015 and 2020). However, compared to the prevalence of kelp farming in Asian countries, there is still significant potential for further growth of the kelp mariculture industry in the United States, specifically in the Gulf of Maine region. In one study, the US EEZ is estimated to have four times the suitable sea space for macroalgae farming compared to China (Liu et al., 2023). The proposed wave-powered water pump to enhance kelp mariculture may help increase productivity for this growing industry.

In 2022, the worldwide algae industry's estimated value was $17 billion USD (FAO, 2024). This translates to approximately $0.47 USD per wet kilogram of algae, which includes both macroalgae (seaweeds) and microalgae. The price in the United States, however, appears to be somewhat higher and can have a wide range. In 2024, Maine reported a marine algae harvest of 463,420 wet kilograms that was valued at $653,886 USD, resulting in a farm price per wet kilogram of macroalgae of approximately $1.41 USD (Department of Maine Resources, 2020). In 2018, a mariculture development plan published by the Alaskan Fisheries Development Foundation estimated that within 20 years a kelp industry could produce 21,772,434 wet kilograms a year and be valued at $15.7 million USD. This would value a wet kilogram of kelp at approximately $0.72 USD (McDowell Group, 2018). Macroalgae pricing depends upon location and added value processing methods. Table 2 provides a summary of the macroalgae price ranges.

Kelp harvests are often reported in wet weight, or as freshly harvested kelp that retains its natural water content. Through processing, kelp may be sold in dehydrated form, and reported as dry weight. Converting from wet weight to dry weight is important for biomass estimates and price comparison. The wet-to-dry ratio of *S. latissima* grown in Gulf of Maine has been measured at approximately 8:1 (averaged over growth season) (Grebe et al., 2021). Other proposed wet-to-dry ratios for sugar kelp include 8.55:1 (Gevaert et al., 2001). Wet-to-dry *S. latissima* ratios tend to depend upon stage of growth season, available nutrient concentrations, and other factors (Sunniva et al., 2020, Reid et al., 2013). The more conservative weight ratio is used to estimate the price of kelp in Section 2.4.1 in lieu of utilizing uncertainty analysis.

The typical yield of an offshore *S. latissima* farm reported in the literature varies widely as shown in Table 3. The typical yield varies from 1 to 45 dried metric tons per hectare per year (DMT ha^{-1} yr^{-1}). This large range depends upon several factors, such as farming style, which includes the depth at which the kelp lines are kept, outplanting and harvest dates, and the planting density (Sanderson et al., 2012; Forbord et al., 2020). Environmental factors also play a major role in determining the biomass yield. The environmental factors most likely to effect the yield include temperature, irradiance, available nutrients, currents, salinity, and exposure to waves and storms (Peteiro and Freire, 2012;

1 Depth-cycling differs from artificial upwelling in that it physically moves kelp lines to greater depths to encounter nutrient-rich and colder water, preferably during night time, and moves them back near the surface during the day for photosynthesis.

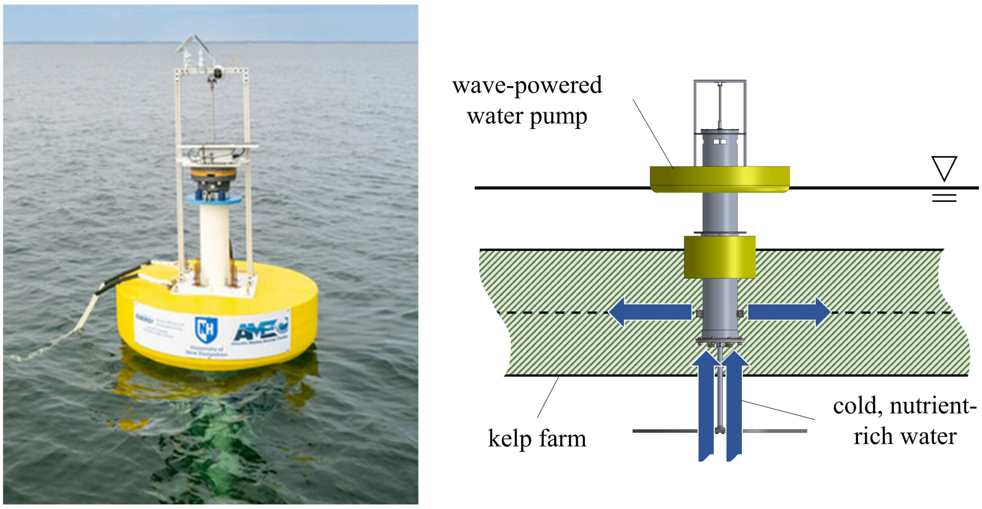

FIGURE 1
Left: A wave-powered water pump deployed during ocean test to benchmark performance and validate numerical model (Kimball et al. 2025). Right: A wave-powered water pump design (Kimabll and Wosnik 2025) shown conceptually operating within a kelp farm (green cross-hatched area). Blue arrows represent deep water brought to the surface via artificial upwelling for distribution into the kelp farm. Not to scale.

TABLE 1 Summary of worldwide macroalgae harvest.

Country/ region	Species grown	2022 yield [wet metric tons]	% of global total	% farmed	Source
Global total	N/A	38 x 10^6	100%	97%	(FAO, 2024)
China	*Saccharina japonica, Gracilaria spp, Porphyra spp*	22.8 x 10^6	60%	99%	(FAO, 2024; Zhang et al., 2022)
North America	*Ascophyllum nodosum, Saccharina latissima*	0.5 x 10^6	1.4%	5%	(FAO, 2024, Zhang et al., 2022; Robidoux and Good, 2023)

Sanderson et al., 2012; Forbord et al., 2020; Broch et al., 2019). In the latitudes closest to Maine's coast (ranging from 41.1 to 45.1°N), the average biomass yield from Table 3 is approximately 9.1 DMT ha^{-1} yr^{-1}. This value is used to benchmark the result of the kelp growth model without artificial upwelling (see Section 3.3.2). In higher latitudes, the biomass yields are typically higher; from the farms in Table 3, these average yields are 24.5 DMT ha^{-1} yr^{-1}. This latitude dependent correlation is likely due to differing environmental variables such as cooler water temperatures, higher seasonal light levels and nitrate concentrations (Peteiro and Freire, 2012; Sanderson et al., 2012; Forbord et al., 2020; Broch et al., 2019).

The ocean is a dynamic and interconnected ecosystem, and when long-term artificial upwelling is introduced, there can be several ecological impacts worth considering. Artificially upwelling deep sea water for enhancing macroalgae growth and sequestering carbon dioxide has been modeled for three species of macroalgae found locally in Hawaiian waters (Chambers, 2022). The study determined that a large-scale, offshore farm utilizing deep sea water for nutrient enhancement would sequester more carbon dioxide than it produced for each of the three species (Chambers, 2022). However, the vertical depth from within the water column that the deep water is sourced is critical in reaching that determination. If the deep water is sourced below the mixed layer depth, then more carbon dioxide is produced during this process than sequestered (Chambers, 2022). In this case study in the Gulf of Maine, where the depth is relatively shallow on a coastal shelf, the mixed layer depth becomes fully mixed seasonally. Therefore, the concern of upwelling deep ocean stored carbon dioxide is negligible (Hopkins, 2025). However, if artificial upwelling is applied to an area of the ocean where the intake depth is below a region which is fully mixed seasonally, it may cause the release of carbon dioxide to the atmosphere that is premature in the natural deep ocean carbon cycle.

Environmental consequences due to long term artificial upwelling not considered in the study may include harmful algal blooms, altered microbial and ecological communities, trophic restructuring, localized acidification, and benthic impacts (Brenckman et al.,

TABLE 2 Summary of macroalgae price ranges.

Country/ region	Type of algae	\$ USD (wet kg)$^{-1}$	Source
Global	Macro and micro	\$0.47	(FAO, 2024)
Maine, USA	Aquaculture seaweed	\$1.41	(Department of Maine Resources, 2015)
Alaska, USA	Kelp	\$0.72*	(McDowell Group, 2018)

*Projected value for 2038.

TABLE 3 Farm grown *Saccharina latissima* biomass yields per hectare per year.

Location	Approximate farm latitude	Biomass yield [WMT ha^{-1} yr^{-1}]	Dry metric ton conversion [DMT ha^{-1} yr^{-1}] (Grebe et al. 2021)	Other notes	Source
Maine, USA	43.7 °N	10	1.2	Fiberglass cultivation lines 150 day season estimate	(Moscicki et al., 2024)
Tjärnö, Sweden	58.8 °N	22.5-27.5	2.6-3.2	240 day season estimate, farmed	(Pechsiri et al., 2016)
Galicia, Spain	43.4 °N	30.2-40.2	3.5-4.7	119 day season, farmed	(Peteiro et al., 2012)
New Brunswick, Canada	45.1 °N	95	11.1	240 day season estimate, farmed near salmon pens	(Reid et al., 2013)
Maine, USA	44.4 °N	96*	11.2	135 day season estimate *S. latissima* forma *angustissima* grown	(Augyte et al., 2017)
Connecticut, USA	41.1 °N	93 - 180	10.9 - 21.1	135 day season estimate two seasons reported	(Kim et al., 2015)
Scotland, UK	58.3 °N	220	25.7	Farmed near salmon pens	(Sanderson et al., 2012)
Frøya, Norway	63.7 °N	383	44.8	134 day season, farmed	(Sharma et al., 2018)

*Assumed 4000 m of cultivation line per hectare (Sanderson et al., 2012).

1980; Schulz et al., 2019). Future field work which involves artificial upwelling should consider permitting requirements, and rigorous environmental monitoring for changing water chemistry and potentially harmful biological impacts.

Tests and models of additional wave-powered artificial upwelling devices have been developed through the past five decades. A comparison of their performance ratios is included in Table 4 (Kimball and Wosnik, 2025). The simulated performance of this wave pump design improved by an order of magnitude from its field tested version, and performs an order of magnitude better than the field tested device by the White et al. research team. It is comparable to other tested devices by the Liu et al. team, and is an order of magnitude smaller than the numerically modeled device by Kirke and field tested device by Vershinskiy et al. These devices are all point absorber WECs. However, other artificial upwelling devices are in development, such as the air lift method. Preliminary field experiments of the air lift method were capable of upwelling water at a maximum rate of 300 m^3 hr^{-1} with an efficiency reported of approximately 3-4% (Fan et al., 2013).

TABLE 4 Published designs and performance of wave-powered artificial upwellers.

Source	Pump diameter	Flow rate [m^3 hr^{-1}]	Performance ratio [m^3 hr^{-1} W^{-1}]
Kimball and Wosnik (2025)	0.43 m	47.4 [a]	25.3 x 10^{-3}
Kimball et al. (2025)	0.10 m	3.8	3.3 x 10^{-3}
White et al. (2010)	0.75 m	16 to 45 [b]	2.4 to 6.8 x 10^{-3}
Kirke (2003)	21.5 m	180,000 [a]	282.3 x 10^{-3}
Liu et al. (1999)	1.2 m	2,232 [a]	26.3 x 10^{-3}
Vershinskiy et al. (1987)	0.30 m	36	267.4 x 10^{-3}

For details on performance ratio calculation see Kimball et al., 2025.
[a]Indicates numerical modeling effort only.
[b]Not directly measured, estimated from temperature data (White et al., 2010).

1.3 Case study site

Figure 2 (GoogleEarth, 2024) shows a map of the study area, which includes the coasts of Maine and New Hampshire in the Gulf of Maine. The case study site is located at the yellow indicator labeled UNH Open Ocean Aquaculture (OOA) site (Irish, 2010), approximately three kilometers south of the Isles of Shoals and eleven kilometers off the coast of New Hampshire. This site was used for open-ocean aquaculture deployments from 1997–2008 (Grizzle et al., 2001; Fredriksson et al., 2004; Irish, 2010), hosted the deployment of several non-grid-connected wave energy converters from 2012–14 (Schakenbach, 2012; Patrick, 2014), and was analyzed according to the IEC Technical Specification 62600–101 for wave energy resource assessment (Meuris and Neary, 2024). The site was selected for this study since multi-year temperature and nitrate concentration measurements at various depths were available, which are critical to the analysis (Irish, 2010).

A "unit" kelp farm of one hectare (100 m x 100 m) is initially considered in the development of a temperature and nutrient transport model. The results are then extrapolated to a one hundred hectare (1,000 m x 1,000 m = 1 km^2), large-scale kelp mariculture operation to calculate kelp biomass yields. The one hundred hectare site is shown as a yellow square in Figure 2, just below the yellow OOA site marker. The data sourced for the transport and kelp growth models are also shown on the map. Measurements of monthly wave conditions, nitrate concentrations, and temperature data were located at the OOA site or nearby (Irish, 2010). The current data were collected from an Acoustic Doppler Current Profiler (ADCP) mounted on a buoy of the National Database Buoy Center (NDBC) located at the white mark, labeled: NDBC 44030

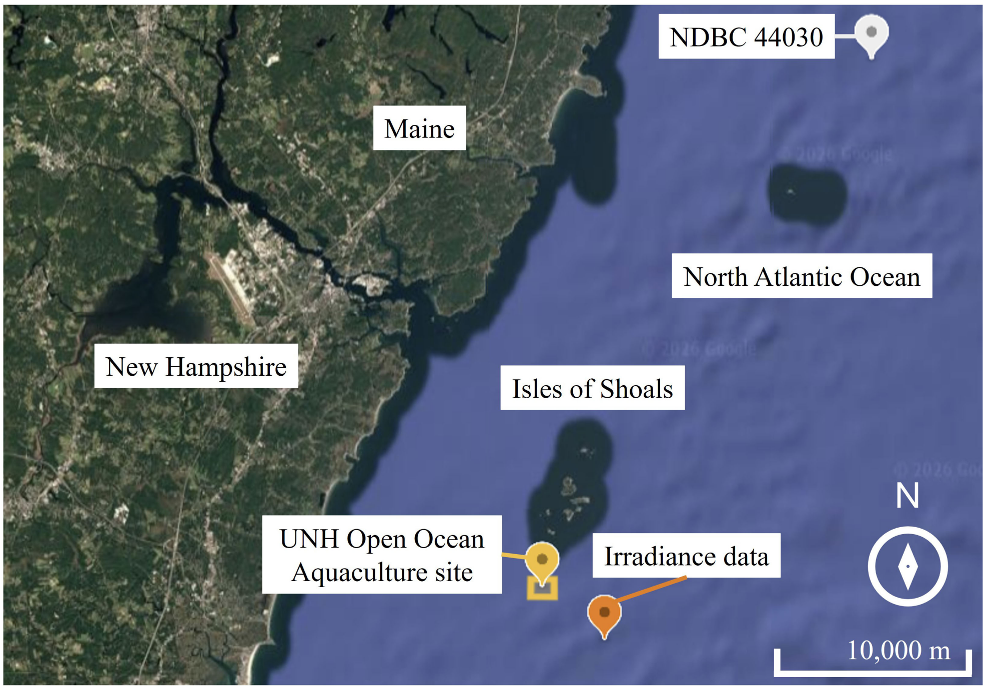

FIGURE 2
Map of the study area (GoogleEarth, 2024), with a yellow marker at the UNH Open Ocean Aquaculture (OOA) site and a white marker at National Data Buoy Center (NDBC) site 44030, the Western Maine Shelf wave rider buoy. The distance between 44030 and OOA is approximately 17 km. The irradiance data is shown by the orange marker centered on the collected area. The one hundred hectare (1 km^2) model kelp farm is shown as the yellow square below the yellow OOA site marker.

(NOAA NDBC, 1971; B01 NERACOOS, 2025). For the nitrate and current data that were collected nearby, from ten to seventeen kilometers away from the site, due to the prevailing currents typically found in the Western Gulf of Maine, these data should be a good representation of the nitrate and currents found at the case study site. The irradiance data are sourced from NASA's Joint Polar Satellite system and Moderate-resolution Imaging Spectroradiometer (MODIS) (MODIS, 2014) for an area that includes the OOA. The orange marker indicates the center of this area. The data for this modeling effort were all collected between 2001 and 2009. The Gulf of Maine is one of the fastest warming oceanic regions with one model estimating that by 2050 the waters will have warmed 1.1-2.4°C compared to average temperatures between 1976 and 2005 (Pershing et al., 2021). For the wave pump impact modeling effort, this indicates that the temperature results may be warmer than what is reported here for present day or future aquaculture farms. Additionally, it may make the artificial upwelling even more effective at reducing surface temperatures due to the warming phenomena.

Temperature data utilized in this study were acquired from 2001 to 2008 at the OOA site by Irish et al (Irish, 2010). The approximate coordinates for the site are 42.94°N and 70.63°W. These data were taken at 0.75 m, 22 m, and 53 m depth, and reported as weekly averages. The temperature was measured via Sea-Bird MicroCat CTD at the surface, and two Sea-Bird SEACAT both at the intermediate and lower depth locations, all located on a common moored structure. The accuracy of the Sea-Bird MicroCat and SEACAT are ± 0.002°C and ± 0.005°C respectively, as reported by the manufacturer. These values likely represent conservative estimates of uncertainty, since the measurements are reported as weekly averages comprising seven years of measurements. Nitrate concentrations were measured separately via Niskin bottle during monthly shipboard transects approximately 10 km northeast of the OOA site. These samples were taken between 2004 and 2009, and were divided into three vertical depth regimes, 0 to 2 m, 10 to 25 m, and beyond 25 m depth. The water samples were processed with 0.22 μm filters, preserved with chloroform, and frozen until analysis. Analysis was completed at the UNH Water Quality Analysis Laboratory using a SmartChem®200 Discrete Analyzer. The nitrate Method Detection Limit was 0.004 mg N L^{-1}, the mean Relative Percent Difference of laboratory duplicates was 0.3%, and the mean recovery of the Laboratory Control Sample was 96.3% (Hunt, 2026). This indicates that the nitrate uncertainty with a 95% confidence interval is ±7.4%.

Irish et al. argued that due to the prevailing currents in the Western Gulf of Maine region, the nitrate samples should be representative of the case study site and visually curve fitted and smoothed the data to obtain weekly averages (Irish, 2010). The weekly average temperature and nitrate data are shown in Figure 3, and show significant seasonal variability in surface, mid-water and deep water values. The uncertainty values for the temperature measurements are not visible in the plot at the scales shown, and the uncertainty values for nitrate are shown on the plot in shaded regions.The water temperature near the surface increases in summer months, while remaining lower at depth. A similar, but inverse trend is observed for nitrate concentration, where near the surface it decreases in the summer months, while remaining higher at depth.

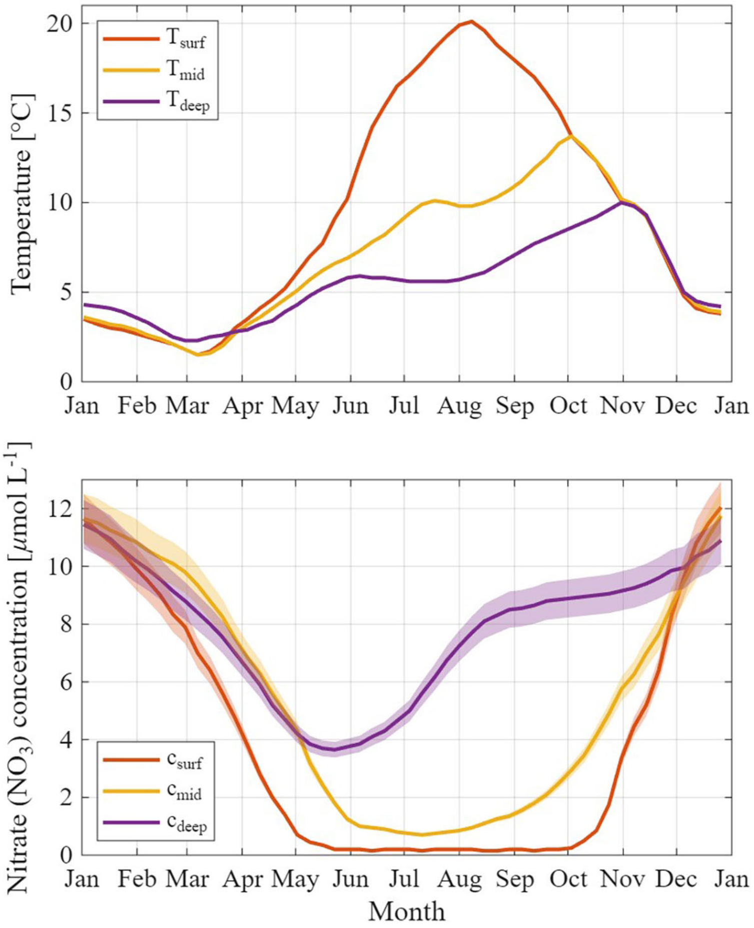

FIGURE 3
Weekly average temperature (T) and nitrate concentration (c) data at the Open Ocean Aquaculture (OOA) site at three different depths: 0.75 m (surf), 22 m (mid), 53 m (deep) taken between 2001 and 2009 (Irish, 2010). Uncertainty for the temperature plot is not visible at scales shown, and for the nitrate plot is shown in shaded regions (Hunt, 2026).

Laboratory studies found that water temperature differences of 4°C can have significant impacts on the health and yield of North Atlantic macroalgae species (Bolton and Luning, 1982; Wilson et al., 2015). The optimal survivability temperature range for *S. latissima* is 10 to 15°C, with decreasing survivability above and below these temperatures as indicated by the kelp survivability model in Figure 4 (Bolton and Luning, 1982; Broch and Slagstad, 2012). Kelp survivability decreases rapidly from 15 to 19°C, and it can be seen in Figure 3 that water temperatures near the surface exceed 15°C in the summer months and can reach as high as 20°C in mid-August. With rapidly warming Gulf of Maine water temperatures (Townsend et al., 2023), this adds to the potential for increased kelp survivability when artificial upwelling cools the surface waters.

The impact of temperature on the farmed kelp yield is captured utilizing the kelp growth model, which was developed by Broch and Slagstad in 2012 (Broch and Slagstad, 2012) and is publicly available. The kelp growth model utilizes environmental conditions of temperature, nitrate concentration, current speed, and irradiance. More details on the processing of the surface current and irradiance data, and kelp growth models are included in Section 2.

The measured environmental parameters, such as temperature and nitrate concentration, provide an input to model kelp growth at a farm. Preliminary research indicates that for every additional 1.0 μmol L^{-1} of nitrate made available in a kelp farm, an additional 3.5 DMT ha^{-1} yr^{-1} can be grown in the Gulf of Maine (Moscicki, 2023). By examining data collected by Boderskov et al. in Denmark, the relationship between average nitrate concentration over the out-planting season for *S. latissima* compared with biomass yield indicates an additional 0.6 DMT ha^{-1} yr^{-1} can be grown for every additional 1.0 μM L^{-1} of nitrate (Boderskov et al., 2023). For additional details regarding this correlation, refer to Appendix. Between mid-March and late June, the average difference between the surface and deep water nitrate concentration is approximately 3.2 ± 0.2 μmol L^{-1}, indicating that with upwelling, there is a significant potential to increase available nitrate in a kelp farm and enhance kelp growth. These examples exclusively examined the effect of available nitrate concentration on kelp biomass yield; however, utilizing a combination of the effects of temperature, nitrate concentration, current speed, and irradiance on the kelp growth model can achieve a more comprehensive prediction of kelp yields when subjected to artificial upwelling. The kelp growth model assumes that nitrate is the only limiting nutrient in kelp growth, and neglects the effects of self-shading, self-nutrient uptake, damage due to storms, presence of epiphytes, and grazing pressure (Broch and

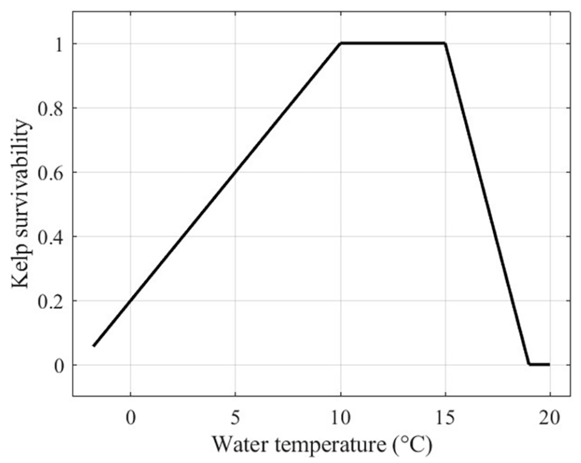

FIGURE 4
Kelp survivability compared with water temperature (Bolton and Luning, 1982; Broch and Slagstad, 2012).

Slagstad, 2012; Strong-Wright and Taylor, 2021). These model limitations could create disagreement between results and reality; however, the model result without upwelling is benchmarked against the average biomass yields from five kelp farms in latitudes similar to the Gulf of Maine in an effort to reduce this uncertainty.

Changes to the ocean water within the case study kelp farm considered in this work with respect to dissolved oxygen and salinity due to upwelling are not expected to significantly affect *S. latissima* growth. The measured range of salinity at the case study location between 2001 and 2008 for all measured water column depths throughout each year was between 29 and 32.5 PSU (Irish, 2010). If upwelling somewhat increased salinity at the kelp farm, this range is within optimal salinity parameters for *S. latissima* (Karsten, 2007; Diehl et al., 2023).

The measured range of dissolved oxygen at the case study location between 2006 and 2008 for all water column depths throughout each year was 7 to 11.5 mg L^{-1} (Irish, 2010). If upwelling somewhat decreased dissolved oxygen at the kelp farm, this range is above the 4.6 mg L^{-1} concentration considered lethal for marine animals (Vaquer-Sunyer and Duarte, 2008). Additionally, kelp has been shown to increase dissolved oxygen by 0.2–2 mg L^{-1} to enhance bivalve aquaculture (Sylvers et al., 2025), and reduced dissolved oxygen conditions may increase photosynthetic rates in some marine macroalgaes, elevating kelp biomass yields (Crowder et al., 2019). The naturally occurring salinity and dissolved oxygen conditions at the case study site near the surface and the bottom are conducive to *S. latissima* growth, and artificial upwelling is unlikely to be detrimental in regards to these environmental parameters.

1.4 Objectives

The objective of this paper is to investigate whether wave-powered artificial upwelling in kelp mariculture could be economically feasible. To begin to answer this, it was estimated how much more kelp can be grown at a mariculture site when utilizing artificial upwelling provided by UNH-AMEC wave-powered water pumps (Kimball and Wosnik, 2025).

The monthly wave conditions at the site were used to simulate wave-powered water pump average upwelling flow rates in a WEC-Sim model that was previously validated during an ocean test (Kimball et al., 2025; Kimball and Wosnik, 2025). Water temperatures and nitrate concentrations measured at varying depths (Irish, 2010) and upwelling flow rates were used as inputs to a simple transport model for a "unit" kelp farm which estimates the resulting water temperature and nitrate concentrations when using artificial upwelling. This simple transport model acts as an initial assessment for transport within a kelp farm, and is not a refined predictive model for this complex and dynamic system. These results are applied to the kelp growth model, along with surface currents and irradiance data available at the case study site to determine what effect the upwelling would have on kelp growth. The estimated value of the additional kelp grown is then compared to the estimated cost of providing wave-powered artificial upwelling to inform economic feasibility. These results are produced iteratively with varied numbers of upwelling devices deployed in the "unit" kelp farm, to optimize the increase in profit to a kelp farm. A concept diagram of multiple wave pumps within a "unit" kelp farm is shown in Figure 5.

This is a first attempt to combine these disparate data sets into a coupled model that can provide a framework to assess potential feasibility of artificial upwelling in kelp mariculture. In future work, this model could be applied to mariculture projects in other locations to aid in the assessment of economic feasibility of artificial upwelling technologies. This model does not capture all of the complexities of large-scale kelp mariculture operations, it simplifies complex ocean fluid dynamics via model coefficients, and uses a range of cost estimates and simple return on investment in the business model. There is significant potential for model refinement, including validation by field experiments or CFD models.

2 Methodology

Section 2.1 describes the process of calculating wave powered upwelling flow rates from a (previously designed) wave-powered water pump and numerical wave energy converter model (Kimball et al., 2025; Kimball and Wosnik, 2025) using wave conditions at the case study location. Next, a one-dimensional temperature and nutrient transport model is developed for the "unit" kelp farm, where the upwelling flow rates are applied to approximate changes in temperature and nutrient concentration due to upwelling at the site. These are used in a growth model for *S. latissima*, developed by Broch and Slagstad (2012), to estimate what increase in kelp growth may be achieved via upwelling. Lastly, the increase in kelp frond area is converted to biomass, and a simple economic assessment determines the potential feasibility (and simple return on investment) of using wave-powered water pumps for a large-scale, model kelp farm in the Gulf of Maine.

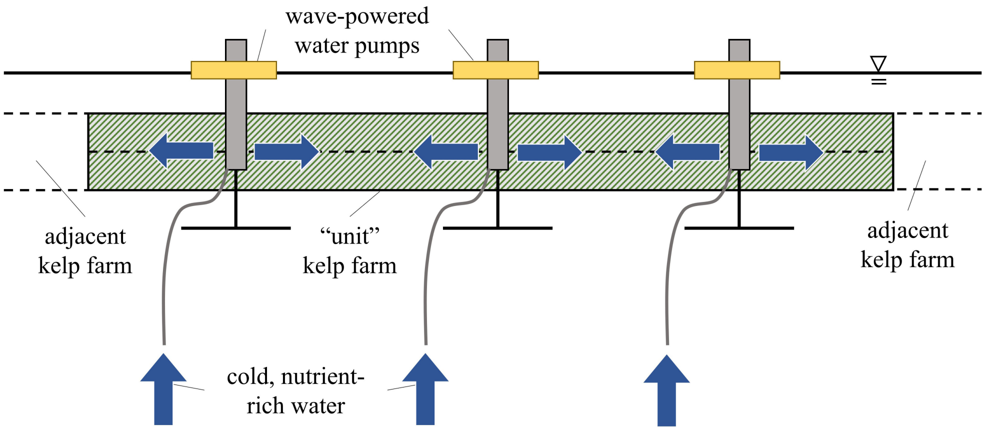

FIGURE 5
Concept diagram of multiple wave-powered upwelling devices deployed in a "unit" kelp farm. Not to scale.

2.1 Calculation of average flow rates by upwelling device using WEC-Sim

A wave-powered water pump is a two-body point absorber that uses relative motion between a wave follower and a spar to upwell water from sub-thermocline depths to the surface. A prototype of the initial concept was ocean tested, from which data were used to validate a WEC-Sim model (Kimball et al., 2025). The validated model was then used to improve the design to increase pump flow rate, be self-righting at all angles, and improve manufacturability (Kimball and Wosnik, 2025). The WEC-Sim model of this improved design was then used to generate wave pump flow rates using local wave conditions as input data for the present study. The simulated flow rate values from the more efficient design (see Table 5, last column) have yet to be validated via laboratory or field tests. For now, a flow rate uncertainty value of ±10% is used, which matches the average percent difference between flow rate values from the ocean test of the prototype and WEC-Sim values (Kimball et al., 2025).

The wave conditions for the OOA site were selected from hindcast data used in the Marine Energy Atlas (Marine Energy Atlas: National Laboratory of the Rockies, US Department of Energy). Uncertainty values are not applied to wave conditions because they are simulated by the global WaveWatchIII model, which relies upon 32 years of data between 1979 and 2010 with three hour temporal resolution and 200 m spatial resolution. Representative monthly energy period and significant wave height data at the OOA are shown in Table 5. Energy period was assumed to be equal to peak period, and these wave conditions were used to simulate the improved wave pump's flow rate response in WEC-Sim (Ruehl et al., 2022). The twelve representative simulations were each run for 1200 seconds in duration with a 1×10^{-4} second time step utilizing JONSWAP wave spectra. The average upwelling flow rate from the wave pump for each wave condition was calculated by using trapezoidal numerical integration (The MathWorks, Inc., 2024) of the output flow rate with respect to time, and averaging over the duration of the simulation:

TABLE 5 **Monthly average wave conditions at the case study location (Marine Energy Atlas) and the corresponding average wave pump flow rates (Kimball and Wosnik, 2025).**

Month	Energy period, T_e[s]	Significant wave height, H_s[m]	Omnidirectional wave power [kW m^{-1}]	Wave pump flow rate [m^3 hr^{-1}]
Jan	5.36	1.04	6.9	43.7 ± 4.4
Feb	5.44	1.12	7.9	49.3 ± 4.9
Mar	5.63	1.21	9.1	51.2 ± 5.1
Apr	5.47	1.15	7.5	49.4 ± 4.9
May	5.15	0.97	4.6	43.8 ± 4.4
Jun	4.90	0.80	2.9	38.1 ± 3.8
Jul	4.70	0.68	1.7	30.5 ± 3.1
Aug	4.90	0.76	2.7	35.7 ± 3.6
Sep	5.43	0.94	4.7	37.7 ± 3.8
Oct	5.52	1.05	6.5	42.8 ± 4.3
Nov	5.43	1.09	7.2	47.9 ± 4.8
Dec	5.37	1.10	8.1	46.7 ± 4.7

$$\overline{\dot{V}}_{upwell} = \frac{\int \dot{V}(t)dt}{T}, \tag{1}$$

where:

$\overline{\dot{V}}_{upwell}$ = average volumetric flow rate outlet from upwelling device [m^3 hr^{-1}],

$\dot{V}(t)$ = instantaneous volumetric flow rate outlet from upwelling device simulated in WEC-Sim as time series data [m^3 hr^{-1}],

T = total simulation time [hr].

To match other model inputs, such as weekly data of temperature and nitrate concentration at the case study site of the one-dimensional transport model, the monthly average wave pump flow rates were then interpolated into weekly average flow rates. To preserve the shape of the monthly flow rate data a piecewise cubic interpolation of the adjacent data was utilized [MATLAB function 'interp1' with 'pchip' as the method (The MathWorks, Inc., 2024)]. The interpolated weekly flow rate values from each monthly wave condition were then used in the one-dimensional transport model to calculate weekly average temperature and nitrate values in the "unit" kelp farm.

The flow rates of the wave pump simulated by WEC-Sim do not include long-term performance, which may degrade due to biofouling or storm conditions. While the first, ocean-tested prototype did include a wire mesh screen with 0.1-inch gaps at the intake to prevent biofouling, there could still be performance degradation due to biofouling.

2.2 One-dimensional temperature and nutrient transport model in a "unit" kelp farm

A representative 100 m × 100 m (= 1.0 x 10^4 m^2 or 1 hectare) "unit" kelp farm located at the OOA site is used in this case study analysis. Kelp farms typically place the growth lines at 2 m depth to reduce loss of kelp due to wave action, while maintaining availability of sunlight at the surface for kelp growth (Flavin et al., 2013; Moscicki et al., 2024). The vertical extent of the "unit" kelp farm "control volume" was set at 2 m (from 1 m depth to 3 m depth), which was chosen by matching longer, average lengths of the kelp at harvest (approximately 1–2 m (Augyte et al., 2017)). Kelp is known to attenuate currents (Lei et al., 2021), and is nearly neutrally buoyant (Vettori and Nikora, 2017) creating a natural barrier when considering the kelp farm control volume. Additionally this effect helps to justify the use of a one-dimensional model which does not consider horizontal currents (or invokes "periodicity" in a very large kelp farm consisting of many unit kelp farms, see discussion below). As the cold-water is introduced to the kelp farm in a direct feed, the kelp blades may act as a natural barrier, reducing the effects of horizontal advection. Selecting a large vertical extent of the farm creates a larger kelp farm control volume, which results in more conservative estimates of achievable nitrate concentration and temperature within the kelp farm due to upwelling. While defining a control volume for a kelp farm and estimating temperatures and nitrate concentration at its boundaries from available data is an approximation, it allows for useful analyses of the control volume.

When the "unit" kelp farm is scaled up to a large scale kelp farm (see concept in Figure 5), surface currents, due to tidal periods or otherwise, may advect the cold-water to adjoining kelp farms, which would gain the benefit of the upwelled waters. Therefore in very large scale kelp farms, the horizontal advection due to surface currents may not adversely effect the modeled results.

The "unit" kelp farm and the available environmental data (Irish, 2010) at the case study site are used in a one-dimensional model to approximate the steady state temperature and nitrate concentration within the farm with a wave pump operating under given wave conditions. The model is assumed to be steady state because the wave pump operates nearly continuously via wave power. Only vertical variations and fluxes are considered in the model, and horizontal ocean currents are not considered at this stage. Temperature and nitrate concentration are assumed to be uniformly mixed within the kelp farm, without the effects of buoyancy, and are assumed to both be passive scalars. A one-dimensional transport equation for temperature is derived from conservation of energy principles, and the transport equation for nitrate concentration is of the same form.

While uniform temperature and nitrate concentration in this large volume are not achievable in practice, the model results should provide a first-order estimate. Targeted introduction of upwelled water along the kelp grow lines may provide higher concentrations of nitrate and lower temperatures locally to the kelp. This can be accomplished with the diffuser system at the outlet of the wave pump. A diffuser system which reduces buoyancy effects, and directly feeds the upwelled water to the kelp is currently in development, and will be described in future works.

The one-dimensional transport model is based on conservation of mass and energy. This simple model is a first-order assessment, and should be strengthened by more rigorous modeling and field validation in future work. The inflow (via upwelling) has the temperature and nitrate concentration of deep water and the outflow (at upper and lower farm boundaries) has the steady state mixed temperature and nitrate concentration of the kelp farm. For the steady-state model, the mass flow rate into and out of the control volume must be equal, and conservation of mass with the kelp farm becomes:

$$\left.\frac{dm}{dt}\right|_{C.V.} = \dot{m}_{in} - \dot{m}_{out} = 0, \text{or} : \dot{m}_{in} = \dot{m}_{out} = \dot{m} \tag{2}$$

or, neglecting density variations, Equation 2 becomes:

$$\dot{V}_{in} = \dot{V}_{out} = \dot{V}, \tag{3}$$

In Equation 3, the inflow $\dot{V}_{in}$ is the average upwelling flow rate from the wave pump and is equal to $\overline{\dot{V}}_{upwell}$, defined in Equation 1. Throughout the remainder of this work, the flow rate from the upwelling device will be simply referred to as $\dot{V}$.

Once the "unit" kelp farm control volume has reached steady state, the energy within it will not change, and energy transport into and out of the "unit" kelp farm must be equal. Conservation of energy for the kelp farm can be written using the first law of thermodynamics for open systems as:

$$\frac{dE}{dt}\bigg|_{C.V.} = 0 = \dot{Q}_{diffuse} + \dot{Q}_{upwell} - \dot{Q}_{advected} \tag{4}$$

This energy balance assumes that the work done within the system is zero, and that the differences in kinetic and potential energy of flows in and out of the system can be neglected. $\dot{Q}_{upwell}$ and $\dot{Q}_{advected}$ represent net flow in and out of the control volume, whereas $\dot{Q}_{diffuse}$ represents turbulent diffusion at the boundary without net flow in and out of the control volume. Figure 6 shows the control volume of the representative "unit" kelp farm, including depths at which temperature and nitrate concentration were measured, and energy flows (not to scale).

The rate of energy associated with the upwelled water can be described by the upwelled water's enthalpy, h_{in}, with $dq_{upwelled} = dh_{in} = c_p dT$ (with $\dot{Q} = \dot{m}q$). Similarly, the rate of energy associated with the advected water (pushed out of the control volume) can be described by h_{out}, with $dq_{advected} = dh_{out} = c_p dT$. The difference between the two energy flows in and out of the kelp farm control volume can then be written as:

$$\dot{Q}_{upwelled} - \dot{Q}_{advected} = \dot{m}c_p(T_{deep} - T_{farm}) = \rho \dot{V} c_p(T_{deep} - T_{farm}), \tag{5}$$

where:
$\dot{Q}_{upwelled}$ = heat transfer rate due to upwelled water [W],
$\dot{Q}_{advected}$ = heat transfer rate due to advected water [W],
$\dot{m}$ = mass flow rate of upwelled water [kg s^{-1}],
c_p = specific heat capacity of sea water at constant pressure [J kg^{-1} $°C^{-1}$],
ΔT = change in water temperature between upwelled and advected [°C],
ρ = sea water density [kg m^{-3}],
$\dot{V}$ = volumetric flow rate of upwelled water [m^3 s^{-1}],
T_{deep} = (upwelled) temperature measured at 53 m depth [°C],
T_{farm} = (advected) steady state temperature within "unit" kelp farm [°C].

The heat flux entering the control volume due to diffusion of heat from water layers through the upper and lower boundaries of the "unit" kelp farm, $\dot{Q}_{diffuse}$, can be expressed as:

$$\dot{Q}_{diffuse} = \rho c_p A_f J, \tag{6}$$

where:
J = total diffusion temperature flux [$m°Cs^{-1}$],
A_f = area of "unit" kelp farm [m^2].

The heat flux at the boundary can be represented using Fick's Law of diffusion, which for vertical temperature differences in the ocean may be written:

$$J_{boundary} = \alpha_T \frac{dT}{dz}, \tag{7}$$

(Tyrrell, 1964) where:
α_T= turbulent vertical eddy diffusivity [m^2s^{-1}],
dT = vertical temperature difference [°C],
dz = vertical distance between different temperatures [m].

Here the dispersion coefficient, α_T, for Equation 7 is the turbulent vertical eddy diffusivity, or turbulent diffusion, which represents the rate of turbulent mixing of momentum, heat or scalars across a fluid layer. It originates from the Reynolds-Averaged Navier–Stokes (RANS) approach, where turbulent mixing processes are modeled using mean gradients (of momentum, heat, etc.), analogous to molecular diffusion processes, combined with an "eddy diffusivity" to address the closure problem (Davidson, 2015). While not an actual physical property, turbulent eddy diffusivity allows turbulent mixing to be quantified – in an average sense. Eddy diffusivity is significantly larger than molecular diffusivity (for momentum, heat, or concentration). In the upper ocean it is several orders of magnitude larger depending on wave and wind conditions (Pawlowicz and Yerubandi, 2024). Other one-dimensional transport models for the ocean, e.g., those developed for oil droplets (Boufadel et al., 2020) or plastic particles (Kukulka et al., 2012), also utilize vertical eddy diffusivity derived from wind data since wave induced turbulent motion at the ocean surface dominates transport processes. Vertical eddy diffusivity varies

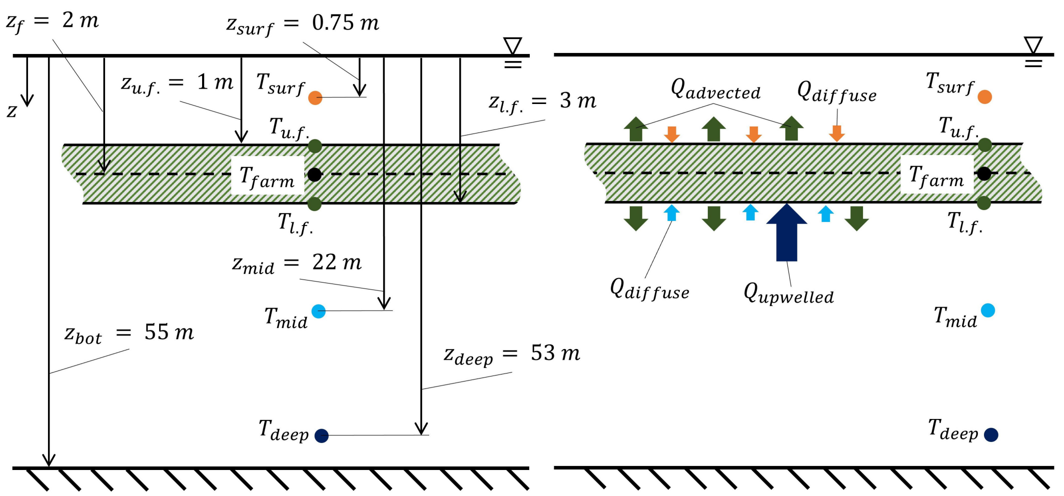

FIGURE 6
Section view of "unit" kelp farm at Open Ocean Aquaculture (OOA) site, shown by boxed green dashed lines. [Left]: Diagram with depths given for one-dimensional (vertical) modeling of temperature and nitrate. [Right]: Diagram with representative heat fluxes shown for one-dimensional transport model. Not to scale.

widely throughout the oceans; however, direct measurements of vertical eddy diffusivity throughout the ocean are approximately 1 x 10^{-5} m^2 s^{-1} (Talley et al., 2011). For the model developed here, weekly average values of vertical eddy diffusivity are approximated as orders of magnitude ranging from 1×10^{-5} to 1×10^{-4} m^2 s^{-1}, which covers seasonal variability at this shallow depth, shallow coastal shelf region in the Gulf of Maine (Benitez-Nelson et al., 2000; Townsend and Larsen, 1992; Levin et al., 2022). Measured hourly or daily values of vertical eddy diffusivity in the Gulf of Maine have been measured at multiple magnitudes higher (typically associated with winter storm events); however, the weekly average estimate is lower than these higher values. The model is evaluated using both the upper and lower bounds to provide a reasonable range of modeled values.

Linear interpolation was used to approximate steady source values at the upper and lower farm boundaries from the measured values at 0.75 m (surface) and 22 m (intermediate) depths for both temperature and nitrate. The linearly interpolated temperatures are described by:

$$T(z) = \frac{T_{mid} - T_{surf}}{z_{mid} - z_{surf}}(z - z_{surf}) + T_{surf}, \tag{8}$$

where:

$T(z)$ = linearly interpolated temperature at either the upper or lower boundary of the "unit" kelp farm control volume [°C]

T_{mid} = weekly average temperature measured at intermediate depth [°C]

T_{surf} = weekly average temperature measured at the surface [°C]

z_{mid} = depth of intermediate measurement [22 m]

z_{surf} = depth of surface measurement [0.75 m]

z = depth of either upper or lower boundary of "unit" kelp farm [1 m or 3 m]

By using Equation 8, the diffusion fluxes at the upper and lower boundaries of the farm can be expressed as:

$$J_{u.f.} = \alpha_T \frac{T_{u.f.} - T_{farm}}{z_f - z_{u.f.}}, \tag{9}$$

$$J_{l.f.} = \alpha_T \frac{T_{l.f.} - T_{farm}}{z_{l.f.} - z_f}, \tag{10}$$

where:

$T_{u.f.}$ = linearly interpolated temperature at the upper boundary of the "unit" kelp farm control volume [°C]

$T_{l.f.}$ = linearly interpolated temperature at the lower boundary of the "unit" kelp farm control volume [°C]

$z_{u.f.}$ = depth of upper boundary [1 m]

$z_{l.f.}$ = depth of lower boundary [3 m]

z_f = depth of kelp lines (vertical center of kelp farm) [2 m].

By adding these expressions for diffusion fluxes together (Equations 9, 10), and substituting the result for J in Equation 6, the combined heat flux due to diffusion can be expressed:

$$\dot{Q}_{diffuse} = \alpha_T A_f \rho c_p \left(\frac{T_{u.f.} - T_{farm}}{z_f - z_{u.f.}} + \frac{T_{l.f.} - T_{farm}}{z_{l.f.} - z_f} \right), \tag{11}$$

Substituting Equations 5 and 11 into Equation 4 and simplifying yields:

$$\dot{V} T_{deep} + \alpha_T A_f \left(\frac{T_{u.f.} - T_{farm}}{z_f - z_{u.f.}} + \frac{T_{l.f.} - T_{farm}}{z_{l.f.} - z_f} \right) = \dot{V} T_{farm}, \tag{12}$$

Rearranging Equation 12 to solve for temperature at the farm yields:

$$T_{farm} = \frac{\alpha_T A_f \left(\frac{T_{u.f.}}{z_f - z_{u.f.}} + \frac{T_{l.f.}}{z_{l.f.} - z_f} \right) + \dot{V} T_{deep}}{\alpha_T A_f \left(\frac{1}{z_f - z_{u.f.}} + \frac{1}{z_{l.f.} - z_f} \right) + \dot{V}}, \tag{13}$$

and through assuming nitrate concentration is a passive scalar, substituting nitrate concentration (c) for temperature (T) yields:

$$c_{farm} = \frac{\alpha_T A_f \left(\frac{c_{u.f.}}{z_f - z_{u.f.}} + \frac{c_{l.f.}}{z_{l.f.} - z_f} \right) + \dot{V} c_{deep}}{\alpha_T A_f \left(\frac{1}{z_f - z_{u.f.}} + \frac{1}{z_{l.f.} - z_f} \right) + \dot{V}}, \tag{14}$$

where a complete summary of variables is shown in Table 6.

The values for the variables in Equations 13 and 14 are given by historical data sets (Irish, 2010; Talley et al., 2011), numerically modeled wave pump flow rate (see Section 2.1), or defined by the representative "unit" kelp farm. The weekly average water temperature and nitrate concentrations within the "unit" kelp farm are then calculated with and without the wave-powered wave pump in operation throughout the year in weekly averages. These are utilized in the kelp growth model to determine the kelp frond area with and without upwelling. There is no time step for this part of the model,

TABLE 6 Summary of variables used in one-dimensional transport model.

Variable	Description and value
T_{farm}	= steady state temperature within "unit" kelp farm [°C]
α_T	= turbulent vertical eddy diffusivity [$1 \times 10^{-5} - 1 \times 10^{-4}$ $m^2 s^{-1}$]
A_f	= area of "unit" kelp farm [1×10^4 m^2]
$T_{u.f.}$	= linearly interpolated temperature at upper edge of kelp farm volume [°C]
$z_{u.f.}$	= depth of upper boundary of kelp farm [1 m]
z_f	= depth of kelp lines (vertical center of kelp farm) [2 m]
$T_{l.f.}$	= linearly interpolated temperature at lower edge of kelp farm volume [°C]
$z_{l.f.}$.	= depth of lower boundary of kelp farm [3 m]
$\dot{V}$	= average volumetric flow rate from wave pump [$m^3 s^{-1}$], for values refer to Table 5
T_{deep}	= temperature measured at 53 m depth [°C]
c_{farm}	= steady state concentration of nitrate within kelp farm [$\mu mol L^{-1}$]
$c_{u.f.}$	= linearly interpolated concentration of nitrate at upper edge of kelp farm volume [$\mu mol L^{-1}$]
$c_{l.f.}$	= linearly interpolated concentration of nitrate at lower edge of kelp farm volume [$\mu mol L^{-1}$]
c_{deep}	= concentration of nitrate measured at 53m depth [$\mu mol L^{-1}$]

For values not given in the table, refer to Appendix.

instead it is solved iteratively with averaged weekly values so that the outputs may be used as input to the kelp growth model. Uncertainty in the model is created by utilizing ranges of flow rates, vertical eddy diffusivity, temperature and nitrate. These ranges are defined as ±10% for flow rate, a range of 1×10^{-5}–1×10^{-4} m^2s^{-1} for vertical eddy diffusivity, instrument manufacturer provided accuracy of ±0.002°C for surface temperature values, ± 0.005°C for intermediate and deep water temperature values, and laboratory uncertainty of ±7.4% for nitrate concentrations. The upper bound of the model utilizes the larger flow rates, smaller eddy diffusivity, lower temperature, and larger nitrate values, and the lower bound is defined by the inverse of each. These uncertainties are applied in these parameter combinations because the first combination generally benefits kelp growth, and the second combination does not.

2.3 Kelp growth model

First developed by Broch and Slagstad in 2012 (Broch and Slagstad, 2012), this growth model for *S. latissima* depends upon environmental conditions of temperature, nitrate concentration, current speed, and irradiance. The model has since been tested for North Atlantic conditions with good results (Broch et al., 2013; Broch et al., 2019; Molen et al., 2018), and a publicly available version of the model in the programming language Julia was developed by Strong-Wright and Taylor in 2021 (Strong-Wright and Taylor, 2021). This section includes the procedure for modeling the frond area of a kelp both exposed to upwelling conditions and not. Next, the process for converting the frond area to kelp biomass is reported.

2.3.1 Estimating frond area in a "unit" kelp farm with application of temperature and nitrate weekly average conditions

Utilizing the publicly available kelp growth model, kelp growth was first modeled with temperature and nitrate values without artificial upwelling ($\dot{V} = 0$), and then successively modeled with temperature and nitrate values with artificial upwelling applied using values calculated from Section 2.1. All physiological parameters were selected from Gulf of Maine data. The irradiance data and current data are kept the same in both model runs.

Irradiance data were sourced from NASA's Joint Polar Satellite system and Moderate-resolution Imaging Spectroradiometer (MODIS) (MODIS-aqua ocean color data, 2014). Also known as Photosynthetically Active Radiation (PAR) data, these daily average data spanned coordinates of 42.8958°N to 42.9375°N and 70.5498° W to 70.6340°W in 4 km resolution, and include dates ranging from July 7th, 2002 to June 27th, 2009. These dates were chosen to closely match the time period that the temperature and nitrate data at the OOA site were collected. NASA reports an absolute irradiance uncertainty associated with 5% of each reported measurement (MODIS-aqua ocean color data, 2014). Since seven years of daily $\overline{PAR}_0$ data are averaged into weeks (49 samples per week), the uncertainty is represented in Equation 15.

$$\pm\,\overline{PAR}_0 = \frac{\pm s}{\sqrt{N}} = \frac{\pm 5\,\% \times \overline{PAR}_0}{\sqrt{49}}, \tag{15}$$

where:

$\pm\, s$ = single measurement uncertainty

N = Number of samples over averaging interval [49 samples].

PAR attenuation due to depth was calculated using diffuse attenuation coefficient, $K_d(490)$, as follows:

$$\overline{PAR}_z = \overline{PAR}_0 \exp(-K_d z), \tag{16}$$

(Morel, 1988) where:

$\overline{PAR}_z$ = average PAR adjusted for depth and measured diffuse attenuation coefficient [μmol m^{-2} day^{-1}]

$\overline{PAR}_0$ = average PAR measured at the surface [μmol m^{-2} day^{-1}]

K_d= diffuse attenuation coefficient [m^{-1}] z = vertical depth into water column [2 m].

Diffuse attenuations coefficients, used in Equation 16, were also collected by NASA's MODIS (MODIS-aqua ocean color data, 2014) for the same dates and areas as the irradiance data. A vertical depth of 2 m was chosen to adjust the PAR data, since this is the typical depth that kelp lines are kept.

Irradiance data were sorted into year-days, year-weeks, and each year-week was averaged. The matching year-weeks over the span of the seven year data set were then averaged. This yielded a weekly average PAR measurement at the case study location, which was then applied to the kelp growth model. Data were interpolated into fifty-two weeks of data to match the other inputs to the model, utilizing the same method of interpolation applied to the flow rate data. Units of PAR are in μmol m^{-2} day^{-1}.

The ocean surface current data were sourced from moored buoy, NDBC Station 44030 (NOAA NDBC 1971; B01 Realtime Doppler, 2025), which is located at coordinates 43.179°N, 70.426°W approximately 17 km northeast from the OOA site. Current data were measured using an ADCP, and spanned dates from July 15th, 2001 to July 4th, 2009. These data were acquired at a rate of approximately 30 samples per hour in two orthogonal directions. The magnitudes of the current data were averaged for each year-week, then sorted and averaged similarly to the irradiance data. The current speed was measured at 2 m depth, which matches the depth of the kelp growth lines in the case study farm. Units for the current velocity are in m s^{-1}. The uncertainty of a single current measurement is ± 2 cm s^{-1} (Chereskin and Harding, 1993); however, since data are averaged into weekly values over a period of approximately seven years (30 samples per hour, 24 hours per day, 7 days per week, and 7 years of data), the weekly average current uncertainty is ± 0.01 cm s^{-1}. Uncertainty is calculated via Equation 17. Refer to Appendix for PAR, K_d, and surface current data used in kelp growth model.

$$\pm\, u = \frac{\pm s}{\sqrt{N}} = \frac{\pm 2}{\sqrt{35280}}, \tag{17}$$

where:

$\pm\, u$ = current uncertainty measurement [cm s^{-1}]

$\pm\, s$ = single measurement uncertainty [cm s^{-1}]

N = Number of samples over averaging interval [35280 samples].

The kelp growth model requires initial conditions for an individual kelp frond. These initial conditions were assigned as follows: frond area of A = 0.1 dm^2, nitrogen and carbon content of N = 0.022 g N (g sw)$^{-1}$ and C = 0.3 g C (g sw)$^{-1}$ respectively. These initial conditions match simulations created by both Broch et al. (2013), and Strong-Wright and Taylor (2021), who showed convergence and insensitivity of the model to a broad range of initial conditions. The model was set to begin on the 276th day of the year, or during the first week of October, when water temperatures at the OOA site begin to drop below 15°C for the fall season, indicating an acceptable time to begin out-planting at the kelp farm due to kelp survivability parameters. The model was set to run for one year to forecast one season's worth of growth. It steps in intervals of seven days to match the input data sets. The input data sets were arranged to match the start of the model as the first week in October, since the kelp growth model relies upon photoperiod. Additionally, the model does incorporate tissue age, however it does not include self-shading, epiphyte loading, grazing pressure, or self-nutrient uptake dynamics. Given these limitations, the result for the non-upwelling case is benchmarked against average yields from five kelp farms at similar latitudes to the Gulf of Maine. The parameters used in the respiration model proposed by Broch et al. were also included in this model (Broch et al., 2013). The model produced the individual kelp's frond area over time throughout the season. This change in frond area with the upwelling environmental conditions was next converted to a change in biomass.

2.3.2 Converting kelp frond area from growth model to biomass

The kelp frond area from a growth season at the case study "unit" kelp farm is produced using the kelp growth model both with and without upwelling conditions applied. Next, converting the frond areas from both scenarios to kelp biomass was required for use in the economic model. The number of kelp individuals per meter cultivation line are sourced from Gulf of Maine farm data and are conservative. The kelp dry weight to frond area is a conservative estimate (Broch and Slagstad, 2012). To complete this conversion, the following equation was used:

$$\frac{\text{DMT kelp}}{\text{ha} - \text{season}} = \frac{[\text{frond area}]\,\text{dm}^2}{\text{ind. kelp} - \text{season}} \times \frac{0.6\text{ g dw}}{\text{dm}^2} \times \frac{100\text{ i nd. kelp}}{1\text{ m cult. line}} \times \frac{4000\text{ m cult. line}}{1\text{ ha}} \times \frac{1\text{ kg}}{1000\text{ g}} \times \frac{1\text{ MT}}{1000\text{ kg}}, \tag{18}$$

where:

DMT kelp = dried metric tons (DMT) of kelp

frond area = maximum frond area of an individual kelp for the modeled growth season

$\frac{0.6\,\text{g dw}}{\text{dm}^2}$ = kelp dry weight in grams per unit frond area, see (Broch and Slagstad, 2012)

$\frac{100\text{ ind. kelp}}{1\text{ m cult. line}}$ = number of individual kelp typically found per meter of cultivation line, see (Moscicki et al., 2024)

$\frac{4000\text{ m cult. line}}{1\text{ ha}}$ = length of cultivation lines in case study "unit" kelp farm over an area of one hectare, see (Sanderson et al., 2012)

2.4 Economic model

A simple techno-economic model was described to investigate the potential economic benefit of the wave-powered water pumps in kelp mariculture. This model relies upon the estimated price of kelp and cost of the wave-powered water pumps to explore whether there could be an economic benefit to using artificial upwelling. A range of costs for the wave-powered water pumps are modeled for comparatively assessing feasibility, since actual, bulk production costs for devices have yet to be determined.

2.4.1 Estimating the price of kelp

The monetary value for one dried metric ton (DMT) of kelp is estimated based on data provided by the Department of Maine Resources for farmed marine algae landings from 2024, which stated that the total farmed marine algae were 1,021,667 wet pounds and were valued at $653,886 USD (Department of Maine Resources, 2020). Since the primary farmed marine algae in Maine are sugar kelp (Robidoux and Good, 2023), the monetary value per dried metric ton of kelp can be estimated using the following equation:

$$\frac{\$\text{USD}}{\text{DMT kelp}} = \frac{\$\text{USD}}{\text{wt . lbs . kelp}} \times \frac{8\text{wt . kelp}}{1\text{ dry kelp}} \times \frac{1\text{lbs .}}{0.454\text{ kg}} \times \frac{1000\text{kg}}{1\text{ metric ton (MT)}}, \tag{19}$$

where:

$\frac{\$\text{USD}}{\text{wt . lbs . kelp}} = \frac{653{,}886\text{USD}}{1{,}021{,}667\text{wt . kelp}} = \frac{\$0.64\text{USD}}{\text{wt . lbs . kelp}}$, see (Department of Maine Resources, 2020)

$\frac{8\text{wt . kelp}}{1\text{dry kelp}}$ = wet – to – dry kelp weight ratio, see (Grebe et al., 2021)

The wet-to-dry kelp weight ratio is from a Gulf of Maine farmed study, and while dependent upon many factors, is chosen as the more conservative weight ratio out of published values (Grebe et al., 2021, Gevaert et al., 2001). Because a conservative value is chosen, no uncertainty is applied to this cost estimate in Equation 19. However, it is important to note that the price of kelp fluctuates depending upon market factors which may include end use, processing, geographic region, public policy, product quality, along with many others. This estimate acts as a first-order attempt to begin exploring feasibility of utilizing wave pumps in kelp aquaculture.

2.4.2 Estimating the cost of manufacture for wave-powered water pumps in bulk

The wave-powered water pump design detailed in Kimball and Wosnik 2025 (Kimball and Wosnik, 2025) was used to model the artificial upwelling flow rates. To determine the cost of manufacturing this device, known off-the-shelf (OTS) part costs, and cost estimates for custom parts were summed together. This cost was approximately \$20,000 USD per device. Since this modeling effort assumes many devices are being utilized, bulk pricing would likely reduce these costs. Adding estimates for labor to assemble the devices would increase the cost. It is assumed that existing vessels required for kelp mariculture operations would deploy and maintain the wave pumps, and existing mooring structures for the kelp farm would be dual purpose for mooring the wave pumps. Additionally, the wave pump could be designed to submerge during non-optimal weather to decrease the operational costs associated with deployment and retrieval each year. Therefore, a range of costs for the wave pump are included in the economic model to indicate what costs may be feasible within the kelp mariculture industry. The modeled costs of each wave pump device are: \$5,000, \$10,000, \$20,000, \$30,000, and \$40,000 USD. While the \$5,000 USD device is an unlikely possibility due to device component requirements, and the \$40,000 device is unlikely to be economically feasible due to the maximum achievable additional kelp growth, these two costs are included to illustrate these limits in the techno-economic model. By utilizing materials which have high durability and low corrosion in the marine environment, the lifetime of the device is estimated as twenty years.

The modeled range of device costs are based around the estimated cost of manufacture. However, the costs do not include maintenance and labor for installation and upkeep. These could increase the cost range of the pumps. For now, the estimated cost range remains between \$5,000 and \$40,000 USD to give insight into what cost ranges might be feasible for these devices.

2.4.3 Estimating additional profit for large-scale, model kelp farm with wave-powered water pumps over device lifetime

Utilizing the additional biomass of kelp produced by upwelling and the range of costs of the artificial upwelling devices, the additional profit for a large-scale, model kelp farm is estimated. The techno-economic model assumes the large-scale, model kelp farm is 100 hectares (1 km^2) in size (made up of 100 “unit” kelp farms of 1 hectare each). Inputs to the model include the sale price at the dock for a dry metric ton of kelp (see Section 2.4.1), wave pump device costs and estimated lifetime (see Section 2.4.2), and number of devices deployed per hectare to achieve the change in kelp biomass. The economic model estimates the net profit of a large-scale, model kelp farm by calculating the increase in profit from additional kelp biomass and subtracting the costs of the devices using the following equation:

$$\text{Add. profit} = \left(\frac{\Delta\text{DMT kelp}}{\text{ha} - \text{season}} \times \frac{\$\text{USD}}{\text{DMT kelp}} \times \frac{100\,\text{ha}}{\text{farm}} \times \frac{20\ \text{seasons}}{\text{device life time}}\right) - \left(\frac{\$\text{USD}}{\text{device}} \times \frac{\text{N devices}}{\text{farm}}\right), \tag{20}$$

where:

$\frac{\Delta\text{DMT kelp}}{\text{ha} - \text{season}}$ = see Section 2.3.2

$\frac{\$\text{USD}}{\text{DMT kelp}}$ = \$11,278 USD, see Section 2.4.1 and (Department of Maine Resources, 2020)

$\frac{\$\text{USD}}{\text{device}}$ = see Section 2.4.2.

The N, number of devices, was selected by iteratively solving the one-dimensional transport, kelp growth, and economic models. The number of devices was iterated in each model from one to ten per “unit” kelp farm. The number of devices which maximized the increase in percentage of farm profit while minimizing the return on investment (years) was selected as the most favorable input. This optimization was completed for each of the five modeled wave pump costs. The percent increase in farm profit was calculated by dividing the additional profit generated due to upwelling (Equation 20) by the estimated profit from the same size model kelp farm without upwelling as shown in Equation 21:

$$\%\ \text{increase farm profit} = \frac{\text{Add. profit (with upwelling)}}{\text{Non} - \text{upwelling farm profit}}, \tag{21}$$

where:

Add. profit = see result of Equation 20

Non-upwelling farm profit = Equation 20 used with modifications: N = 0, and estimate of $\frac{\text{DMT kelp}}{\text{ha}-\text{season}}$ from non-upwelling case, see Section 2.3.2

The estimate for years until simple return on investment (ROI) is reached is calculated by using:

$$\text{ROI} = \frac{\left(\frac{\text{N devices}}{\text{ha}} \times \frac{\$\text{USD}}{\text{device}}\right)}{\left(\frac{\Delta\text{DMT kelp}}{\text{ha}-\text{year}} \times \frac{\$\text{USD}}{\text{DMT kelp}}\right)}. \tag{22}$$

The simple ROI calculated in Equation 22 is exploratory, since additional costs are not considered in the device cost range. The labor costs associated with installation and maintenance including repairing storm damage, biofouling, and permitting costs are not considered. The cost of the wave pumps also assume that the kelp farm moorings are configured in such a way that they can be dual use and act as the wave pump moorings.

3 Results and discussion

The results and discussion section is composed of four subsections. These include the WEC-Sim (Ruehl et al., 2022) modeled average flow rates which were used in the temperature and nutrient transport model. The transport model produces estimated changes in temperature and nitrate concentrations at the “unit” kelp farm, which are entered into the kelp growth model. The kelp growth model approximates frond area at the reference farm both with and without upwelling conditions. Finally the biomass conversion from the upwelling condition is used in a simple techno-economic model to estimate the potential feasibility of artificial upwelling in sugar kelp mariculture.

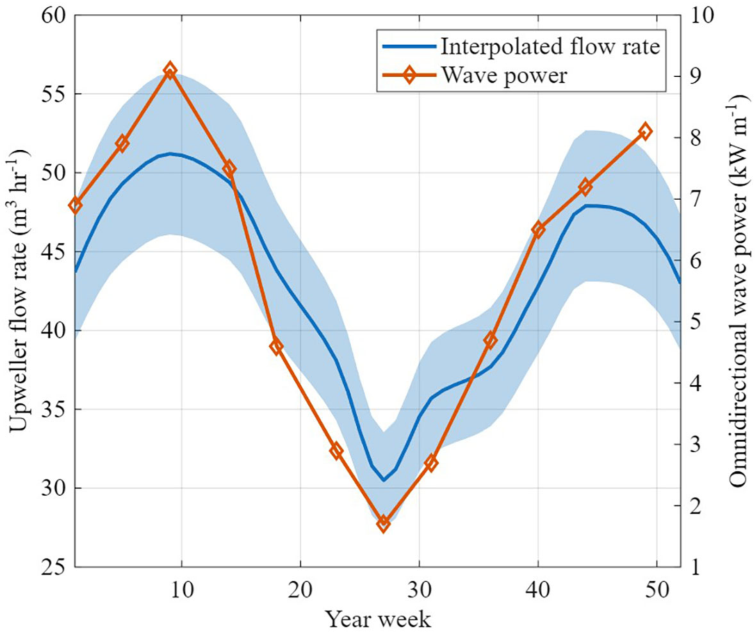

FIGURE 7
WEC-Sim generated wave pump flow rates interpolated to weekly data, and omnidirectional wave power at the OOA site plotted monthly. Wave conditions are used to generate simulated flow rate data, which was then interpolated to weekly values to match site environmental data. Shaded region represents the $\pm$10% of flow rate values to account for model uncertainty.

3.1 WEC-Sim generation of average flow rates by upwelling device

The average flow rates generated by a WEC-Sim (Ruehl et al., 2022) time domain simulation for each wave condition at the OOA are included in Table 5. As the available wave power changes, the flow rate from the wave pump responds accordingly, as seen in Figure 7. Peaks are observed during early spring and late fall, with the lowest values for both flow rate and wave power occurring during the mid-summer season. The highest simulated flow rate of 51.2 ± 5.1 $m^3\ hr^{-1}$ occurred during March, and the lowest of 30.5 ± 3.1 $m^3\ hr^{-1}$ occurred during July. The yearly average flow rate for one device is 43.1 ± 4.3 $m^3\ hr^{-1}$ at the case study location.

These flow rate values have yet to validated beyond the WEC-Sim model. An estimate of flow rate uncertainty may be approximately ±10%, which is shown by the shaded region in the figure. ± 10% is the percent difference of flow rates found during the WEC-Sim validation effort for the ocean tested prototype (Kimball et al., 2025). While the ocean tested prototype has different geometries associated with the device, the core working principles and power-take-off (PTO) operation remain the same between the ocean tested prototype and the in-silico improved design.

3.2 One-dimensional temperature and nutrient transport model

The temperature and nitrate concentration at the OOA "unit" kelp farm site are modeled throughout the year with three wave-powered water pump devices deployed in one hectare of an example farm as shown in Figure 8. For temperature, the largest effect is noticeable in the warm season from June through October when compared to surface values. The temperature at the same depth as the farm without upwelling has an average estimated temperature of 16.3°C ± 0.01°C from June through October (linearly interpolated from measurements). When the upwelling devices are present, the equivalent temperature is 15.3°C ± 0.15°C (maximum), with the largest weekly average modeled temperature decrease of 1.4°C ± 0.15°C occurring the second week of August. Since kelp survivability and growth is highly dependent on the temperature of surrounding waters (Bolton and Luning, 1982), these changes may have an appreciable effect on the kelp biomass yield.

Modeled weekly average nitrate concentration increases at the "unit" kelp farm most noticeably from June through September, when compared to the measured surface values. The nitrate concentration at the same depth as the farm without upwelling has an average value of 0.2 μmol L^{-1} from June through September (linearly interpolated from measurements). With three upwelling devices deployed, this average increases to 0.3 to 1.3 μmol L^{-1} for the same period depending on modeled parameters. Parameter uncertainty is accounted for by assessing the model twice. One run includes 10% larger flow rates, $1 \times 10^{-5}\ m^2\ s^{-1}$ vertical eddy diffusivity, 0.005°C lower temperatures, and 7.4% higher nitrate concentrations. The second run includes 10% lower flow rates, $1 \times 10^{-4}\ m^2\ s^{-1}$ vertical eddy diffusivity, 0.005°C higher temperatures, and 7.4% lower nitrate concentrations. The largest weekly average modeled nitrate increase of 0.01 to 1.4 μmol L^{-1} occurs during the last week of September. This increase in available nutrients, where nitrate has been shown in many studies to be a limiting agent in *S. latissima* growth (Sunniva et al., 2020; Forbord et al., 2021), may also have a positive effect on the growth when applied to the kelp growth model.

This one-dimensional, simplified transport model has certain limitations which should be considered when reviewing these

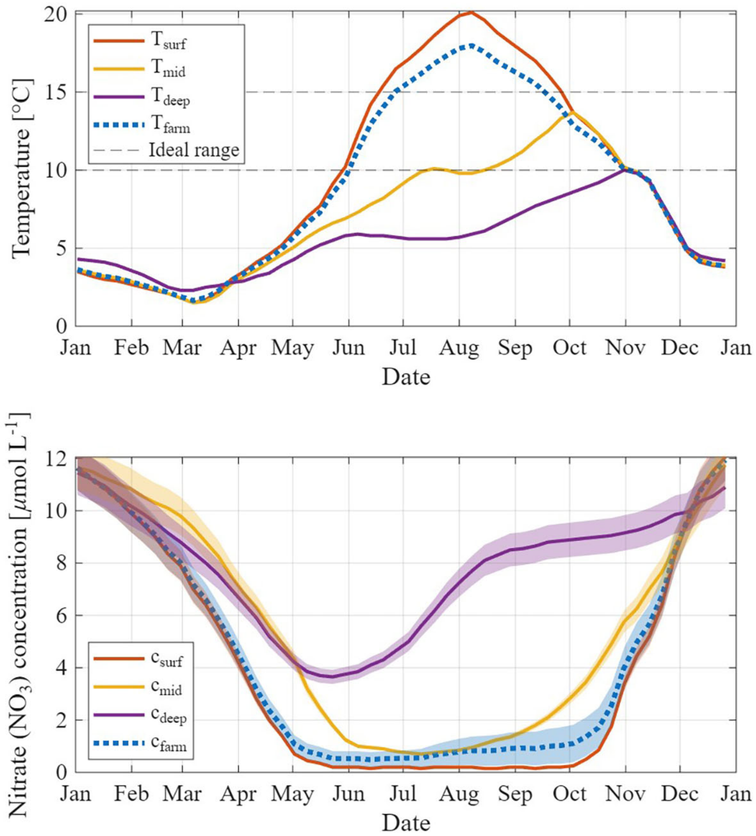

FIGURE 8
Top: temperatures measured at the surface, mid-depth, and deep water locations at the Open Ocean Aquaculture site. Additionally, the steady state temperature within the "unit" kelp farm is shown, modeled with three wave-powered water pump devices deployed (T_{farm}). Temperature uncertainty bounds not visible at scales shown. The ideal temperature range for *S. latissima* is shown by the horizontal dashed black lines. Bottom: nitrate concentration for the same depths and for the "unit" kelp farm (c_{farm}). Shaded regions represent uncertainty of modeled nitrate values at the farm (blue) depending upon input parameters, and nitrate values throughout the water column (orange, yellow, purple) depending on measurements.

results. This first-order estimate is being used as a screening tool, to estimate temperature and nitrate changes at a kelp farm due to upwelling. It does not consider horizontal advection, fluid interactions with kelp blades, tidal effects, impacts and variability of vertical stratification, horizontal mixing, plume spreading, and many others in this dynamic ocean system. The vertical eddy diffusivity and wave pump flow rate are both model parameters with unknown uncertainties. If the attenuation effects from kelp blades are more pronounced, combined with a direct feed between wave pump and kelp grow lines, the model may under-predict the effectiveness of the wave pump impact. This indicates that the modeled wave pump may be more or less effective at achieving the temperature and nitrate conditions reported here at an example kelp farm. A field experiment to test these results should be performed in future works to assess model validity.

Additionally, the model utilizes data collected between 2001 and 2009, which may no longer be representative of the Gulf of Maine conditions, which have been warming faster than many other ocean regions in recent years (Townsend et al., 2023). This may indicate that the cooling effects from artificial upwelling could be even more impactful on sugar kelp mariculture in the Gulf of Maine for present and future kelp farmers.

Long term artificial upwelling may have ecological consequences not considered in this work. While unlikely for the example kelp farm location, in other geographic areas when upwelling is applied, the premature release of carbon to the atmosphere and oxygen depletion could occur. These could have additional chain reactions such as harmful algal blooms, altered ecological communities, localized acidification, benthic impacts and others (Brenckman et al., 1980; Schulz et al., 2019). In future field studies permitting and environmental monitoring will be important in determining whether these effects likely to occur.

3.3 Kelp growth model

The results from the kelp growth model include both the change to an individual kelp's frond area due to upwelling, as well as the extrapolated change in biomass for a large-scale kelp mariculture operation.

3.3.1 Estimating frond area in "unit" kelp farm with application of temperature and nitrate weekly average conditions

The weekly average inputs to the kelp growth model are shown in Figure 9, beginning in October and spanning one year. Temperature at 2 m depth is lowest in early spring, and highest in mid-summer. With the upwelling transport model, temperature

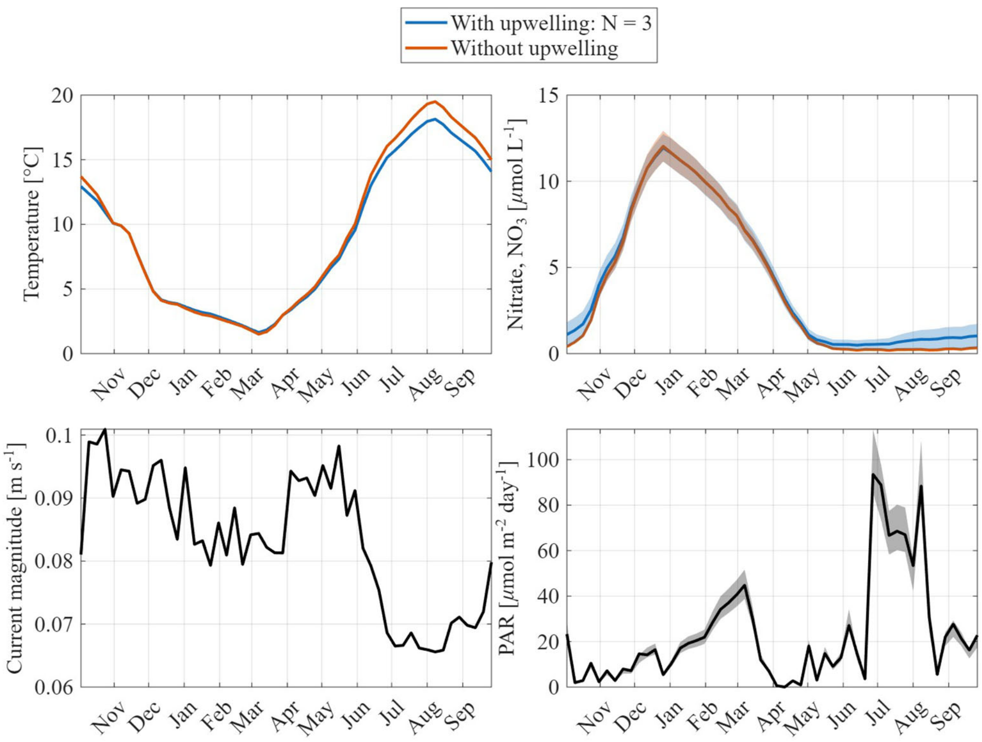

FIGURE 9
Environmental input data at the "unit" kelp farm for an individual kelp frond growth model. Data includes weekly averages over several years for temperature (°C) (Irish, 2010), nitrate (NO_3, μmol L^{-1}) (Irish, 2010), current magnitude (m s^{-1}) (NOAA National Data Buoy Center, 1971), and PAR (μmol m^{-2} day^{-1}) (MODIS-aqua ocean color data, 2014) beginning in October and spanning one year. Temperature and nitrate concentration are modeled with three upwelling devices, shown in blue, and without upwelling applied, shown in orange. The uncertainty for temperature and current magnitudes are not visible at the scales shown. Uncertainty for nitrate is shown with blue and orange shaded for both upwelling and non-upwelling cases respectively. Uncertainty for the irradiance measurement is shown by the gray shaded region.

is lower in June through October. The uncertainty in the temperature measurement is not visible at the scales shown in the figure. Nitrate at the "unit" kelp farm depth shows an inverse relationship, where the highest concentrations are present late fall through spring, when the site is well mixed vertically. The upwelling transport model increases the amount of nitrate available in the spring, summer, and fall to benefit the growth of kelp. The uncertainty in the nitrate measurement was ±7.4%, which is represented by the orange shaded region for the non-upwelling case. The upwelling case shares this uncertainty, mostly over the December to March time frame, where these shaded regions overlap. The upwelling case also has uncertainty associated with vertical eddy diffusivity and flow rate, shown by the blue shaded region most visible from late May to December. This range in nitrate values over this time period is mostly caused by the range of vertical eddy diffusivity analyzed.

The average current speed at 2 m depth varies significantly week to week. There is a general trend of larger current speeds in fall and spring, with the lowest current speed in the summer. Generally, current speed affects the kelp's nutrient uptake rate, where larger currents increase the amount of nutrient uptake, thus increasing growth (Broch and Slagstad, 2012). The uncertainty in the current speed measurement is not visible at the scales shown in the figure. Finally, PAR is lowest in the winter and highest in the summer, and kelp experiences more growth with higher irradiance levels (Sunniva et al., 2020). The PAR data have been attenuated for depth and chlorophyll levels (diffuse attenuation coefficient). This is represented in the data by the increasing PAR levels in early spring, relating to more available sunlight, which quickly decrease in mid-March due to algal blooms. PAR rises again mid-summer when the algal blooms have decreased and high levels of irradiance are present. The gray shaded regions represent the uncertainty associated with the PAR measurement, reported as ±5% for the surface measurement and carried through in the depth and chlorophyll attenuation calculation. These parameter uncertainties will cause the kelp growth model to produce a range of frond area values for the upwelling and non-upwelling cases.

Figure 10 shows the difference in individual kelp frond growth area between a "unit" kelp farm that experiences upwelling throughout the year (with three devices), and one without any upwelling. The difference between the two models relies upon the change in temperature and nitrate concentration available at the farm, while average current magnitude and irradiance levels are kept the same. Uncertainties for the four inputs are also included in the model, shown in the figure by the shaded regions, and are included for both the upwelling and non-upwelling cases. The kelp frond area without upwelling experiences a maximum value of $38.9^{+0.6}_{-0.7}$ dm^2 occurring June 25th, and with upwelling the maximum kelp frond area is $42.6^{+1.3}_{-4.6}$ dm^2, occurring four days earlier on June 21st. With the upwelling devices deployed in the "unit" kelp farm, individual frond growth is modeled to increase by $9.5\%^{+1.6\%}_{-10\%}$, and achieves this larger size a few days earlier than without upwelling.

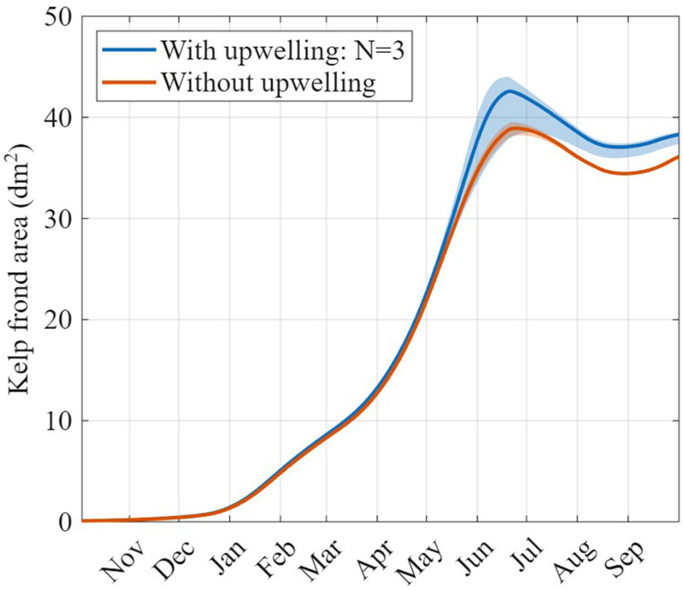

FIGURE 10
Individual kelp frond growth represented by area in square decimeters (dm^2) throughout a year-long growing season beginning the first week in October. The frond area with three upwelling devices per hectare is shown in blue and without upwelling is shown in orange. The shaded regions represent uncertainty within the models for resulting kelp frond area.

This disparity in timing is likely caused by two factors in the kelp growth model. First, the frond growth is dependent upon season (photoperiod), and if more favorable conditions occur sooner in the year (as observed in the upwelling case), this will cause more growth to occur sooner in the year, and create an earlier peak (Broch and Slagstad, 2012; Strong-Wright and Taylor, 2021). Secondly, apical frond loss is accounted for in the frond area model, and this loss becomes exponentially larger as the frond grows due to tissue age, which could lead to a peak and decrease occurring sooner in the year for the larger frond (upwelling) case. The frond area model equation, and some accompanying equations to the model are included in the Appendix.

The uncertainties associated with the kelp growth model frond area results have a wider range for the model with upwelling compared to the non-upwelling case. This uncertainty is associated with the one-dimensional transport model uncertainties, specifically the range of available nitrate concentration created by upwelling. This model is most sensitive to vertical eddy diffusivity, where the range of modeled values results in the wide range of kelp frond area shown in Figure 10. With the upwelling case's modeled uncertainties, there is the possibility for the biomass to decrease by up to 0.5% compared to the non-upwelling case, which points to the potential lack of feasibility for artificial upwelling devices in kelp mariculture. However, given the uncertainties currently attributed to the model, and the potential to increase the yield by up to 11.1%, further field testing should be conducted to validate the model and results prior to making conclusions on artificial upwelling economic feasibility.

The model does not consider self-shading or nitrate self-uptake, which may be a reasonable assumption in low density kelp farms (Strong-Wright and Taylor, 2021). Additionally epiphyte occurrence, grazing, and storm damage are not considered in the model; however, irradiance, photoperiod, current velocity, and tissue age are all considered in addition to temperature and nitrate concentration. This could create some uncertainty in the presented values. The non-upwelling case yield is compared against five average kelp farm yields in latitudes similar to the Gulf of Maine in an attempt to reduce some of this uncertainty.

3.3.2 Converting kelp frond area from growth model to biomass

Converting individual sugar kelp frond area into biomass extrapolated over the "unit" kelp farm yields a harvest for the non-upwelling case of $9.3^{+0.2}_{-0.1}$ DMT ha^{-1} yr^{-1}. This is calculated by substituting the maximum frond area from the kelp growth model in Section 3.3.1 into Equation 18. Since one growing season lasts approximately from beginning of October to the end of June (approximately nine months), one growing season is approximated as being one year. The modeled $9.3^{+0.2}_{-0.1}$ DMT ha^{-1} yr^{-1} of *S. latissima* harvested from the "unit" kelp farm can then be compared to the average harvests of other farms located between 40°N and 46° N in Table 3 (five farms) in an effort to benchmark the modeled value. These yields vary from 1.2 to 21.1 DMT ha^{-1} yr^{-1}, with the average yield of 9.1 DMT ha^{-1} yr^{-1} for these farms. The modeled value of 9.3 DMT ha^{-1} yr^{-1} is very similar to the average benchmark value of 9.1 DMT ha^{-1} yr^{-1}, with a difference of approximately 2%. This indicates that the modeled kelp farm biomass yield without upwelling is likely a good estimate.

When three upwelling devices are applied to the "unit" kelp farm, the *S. latissima* yield increases to $10.2^{+0.4}_{-1.0}$ DMT ha^{-1} yr^{-1}, or an increase of $0.9^{+1.1}_{-0.0}$ DMT ha^{-1} yr^{-1}. This increase is approximately $9.5\,\%^{+1.6\,\%}_{-10\,\%}$ compared to the case study farm without employing upwelling devices. When considering the "unit" kelp farm, the additional biomass yield is modeled as approximately 0–2 additional DMT ha^{-1} yr^{-1} compared with the non-upwelling case.

TABLE 7 Modeled biomass yields with and without artificial upwelling benchmarked against actual yields reported in literature.

Case	Avg. flow rate [m3 hr−1]	Kelp yield [DMT ha^{-1} yr^{-1}]	% yield change (upwelling only)
With upwelling	129.3 ± 10%	$10.2^{+0.4}_{-1.0}$	$9.5^{+1.6}_{-10}$
Without upwelling	N/A	$9.3^{+0.2}_{-0.1}$	N/A
Benchmark farms (Augyte et al., 2017; Peteiro et al., 2012; Reid et al., 2013; Kim et al., 2015; Moscicki et al., 2024)	N/A	9.1 (avg.)	N/A

Clarifying uncertainties in future models will help to determine the economic feasibility of artificial upwelling. These results are summarized in Table 7.

On average throughout the year, the nitrate increase due to three upwelling devices at the farm is 0.3 ± 0.3 μmol L^{-1}. Given the results of the kelp growth model, this indicates that for every additional 1.0 μmol L^{-1} of nitrate, an additional $3.0^{+3.0}_{-0.0}$ DMT ha^{-1} yr^{-1} of kelp may be grown. This value falls within the range estimated by researchers for additional kelp growth due to each additional 1.0 μmol L^{-1} of nitrate, which ranges from 0.6 to 3.5 DMT ha^{-1} yr^{-1} (Boderskov et al., 2023; Moscicki, 2023), respectively). While the results of this study have a wide range when uncertainty is included, they generally align with other approximations made in this field. This ratio of kelp growth to available nitrate is also modeled as a specific case study for the Gulf of Maine location, and likely varies in other geographic regions.

3.4 Economic model: estimating additional profit for large-scale, model kelp farm with wave-powered water pumps over device lifetime

An economic accounting model was developed to estimate the increase in kelp farm profit compared to a return on investment for a given number of devices and a range of potential device cost estimates (see section 2.4.2). When iteratively solving the one-dimensional transport, kelp growth, and economic models for varying numbers of devices in each hectare, a favorable case was selected for each of the five selected device costs as shown in Table 8. The selection criteria included maximizing percent increase in farm profit, and minimizing years until simple return on investment, by referencing Figure 11. For example, for the \$20,000 cost per wave pump device case (yellow circle markers), three upwelling devices per hectare were selected as optimal because it matched both of these criteria better than the other tested cases. The simple ROI for three devices is approximately $6.0^{+70}_{-1.0}$ years for this case, and the increase in farm profit over the device lifetime is approximately $6.6\,\%^{+2.0\,\%}_{-8.7\,\%}$. Four devices would marginally increase the percent of farm profit, but would also increase the years until ROI is reached. After five or more devices are deployed, the increase to farm profit begins to decrease, making these cases less favorable. The shaded regions which color correspond to the markers indicate the uncertainty range associated with each device cost. These regions vary widely, but are consistently approximately +2.0% and approximately -8.7% for the upper and lower uncertainty bounds respectively for percent increase in farm profit for each device cost which utilizes three devices per hectare. This range of values indicates that there is a possibility for economic feasibility when utilizing artificial upwelling, as well as a potential for lack of feasibility. This large range is due mostly to the range of vertical eddy diffusivity modeled, and future work validating the model and performing field tests should help to resolve this uncertainty. Additional non-optimal conditions which could contribute to the lack of feasibility for wave pumps in kelp aquaculture include higher water temperatures, lower nitrate concentrations, lower surface currents, lower irradiance levels, and non-optimal wave pump performance.

TABLE 8 Favorable case for number of devices per hectare for each device cost by maximizing percent increase in farm profit and minimizing years until simple return on investment (ROI) is achieved.

Device cost (\$ USD)	Favorable number of devices	% increase in profit	ROI (yrs)
\$5,000	3	$8.7^{+2.0}_{-8.4}$	$1.5^{+17.5}_{-0.3}$
\$10,000	3	$8.0^{+2.0}_{-8.7}$	$3.0^{+35}_{-0.5}$
\$20,000	3	$6.6^{+2.0}_{-8.7}$	$6.0^{+70}_{-1.0}$
\$30,000	3	$5.2^{+2.0}_{-8.8}$	$9.0^{+105}_{-1.6}$
\$40,000	3	$3.8^{+2.0}_{-8.8}$	$12.1^{+140}_{-2.2}$

The device costs and ROIs shown in Figure 11 are chosen to estimate a potential region of feasibility for artificial upwelling limited by the biological growth model of *S. latissima*. While the \$5,000 USD cost per wave pump device case is unlikely to be feasible due to device component requirements, it is a useful case to consider as it demonstrates how there is a maximum percent growth in farm profit due to upwelling because of the limits to kelp growth. The \$30,000 and \$40,000 cost curves are truncated at six and four devices respectively due to limits placed on the ROI axis, which is set to a maximum of 15 years. With the device lifetime estimated at 20 years, a ROI larger than 10 years is unlikely to be an economically feasible case. Additionally, the negative percentage increase in farm profit (or decrease in profit) are not shown on the ordinate axis since these are economically infeasible. Wave-powered water pump devices which cost between \$10,000 and \$30,000 are most likely to be economically feasible for enhancing yields at a large-scale, model kelp farm if the average or more favorable uncertainty results from the one-dimensional transport model are validated. In this range, using three devices per hectare may maximize the increase in farm profit from 5 to 10%, while minimizing the ROI between three and nine years approximately (see Table 7). If the less favorable uncertainty results are validated, then the wave pump devices may prove infeasible for this case study.

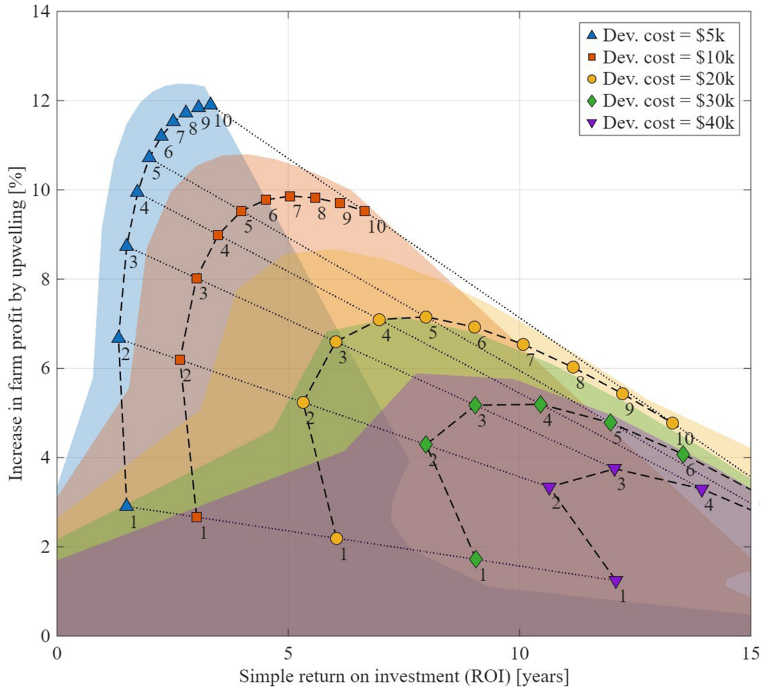

FIGURE 11
Iterative modeling approach for number of upwelling devices per hectare (shown within plot to the right of each marker) and cost for each upwelling device, comparing the years until simple return on investment (ROI) to the percentage increase in farm profit for each case. Shaded regions indicate uncertainty propagated through models which show the range of profits and simple ROI's associated with each device cost and number of devices per hectare. (Table 8 shows data for three devices per hectare).

This techno-economic accounting relies upon assumptions that the device cost ranges do not include costs associated with labor, maintenance, and that storm damage will be limited. It also assumes that vessels and moorings required for the wave pumps are dual use for the kelp farm, to reduce these additional costs.

4 Conclusion

In the Northern hemisphere on shallow, coastal shelves, artificial upwelling during the warmer seasons could be beneficial to kelp farms. This is due to the formation of a thermocline at relatively shallow depths, below which water with colder temperatures and higher nitrate concentrations exist. This deeper water can be upwelled to the surface with wave-powered water pumps. This case study explores the feasibility of utilizing wave pumps within kelp farms within a preliminary modeling framework.

A wave pump used at a "unit" kelp farm (one hectare) may increase the available nitrate and decrease the water temperature during the warmer seasons. When deploying three upwelling devices at the case study location, preliminary modeling implies that the biomass yield at a "unit" kelp farm may increase by approximately $9.0^{+1.1}_{-0.0}$ DMT ha^{-1} yr^{-1} or by approximately $9.5^{+1.6\%}_{-10\%}$. This can be achieved with wave pumps designed to produce an average upwelling rate of 43.1 ± 10% m^3 hr^{-1} throughout the year. As ocean current velocities near the surface can readily overwhelm the wave pump's upwelling flow rates within the "unit" kelp farm, the results obtained here can be considered more representative for a large deployment area of many adjacent kelp farms. These results will require field-scale validation in future work.

The framework presented here combines several models to assess the feasibility of artificial upwelling in kelp mariculture. The coupled models include four major steps. First, a WEC-Sim model provides flow rates based on wave conditions. This WEC-Sim model was validated by flow rate, displacement, and wave data from an ocean deployment of a prototype operating with similar principles. These flow rates are used within the next model, a transport model, that additionally uses water temperatures and nitrate concentrations measured at varying depths to determine how upwelling may change these conditions. Third, a kelp growth model uses these temperature and nitrate inputs along with surface currents and irradiance data to produce biomass yield estimates, which are used as inputs for the final model: a simple economic model to begin assessing wave pump feasibility in kelp aquaculture. This framework can serve as a first-order screening tool. Field validation and more realistic hydrodynamic-biogeochemical modeling should be conducted before drawing stronger conclusions.

The one-dimensional transport model relies upon several assumptions, which may not be representative of an ocean kelp farm. These assumptions neglect the effects of horizontal advection (or invoke periodic boundary conditions among many adjacent unit kelp farms), plume dilution, farm-scale circulation, buoyancy of upwelled water, and attenuation effects of kelp. Most of these effects will require more realistic modeling and testing in an ocean kelp farm for model validation. However, some effects may also be mitigated by design, e.g., by utilizing an appropriate diffuser at the outlet of the wave pump. A diffuser which promotes mixing can reduce the negative buoyancy effects of upwelling cold water into warmer surface waters. The proximity of multiple wave pump outlets to the kelp lines was also not considered in the simple model, and may improve conditions in the vicinity of the kelp. Beneficial diffuser designs for the wave pump outlets will be explored in future work. Since device spacing is much larger than device diameter (47 m >> 2.5 m), the wave pump devices are unlikely to degrade in their hydrodynamic performance when deployed in arrays (Falnes, 2002).

As the kelp mariculture industry continues to grow in the United States, and more locally within Gulf of Maine waters, the ability to utilize kelp as a feedstock for biofuel and bio-plastics, food crop, and many other applications, also increases. When utilizing kelp in this way, there is a decrease in atmospheric carbon emissions, and an additional benefit of sourcing this feedstock from local waters. Wave-powered water pumps which act as artificial upwelling devices could potentially increase biomass yields of farmed kelp, without increasing farmed area or significantly increasing operational costs. The feasibility study presented here relies upon several assumptions for the design and deployment of the wave pumps. First, the device would share deployment vessels and moorings with existing kelp farms to reduce costs. Second, the wave pumps would have high storm survivability. This could be achieved by designing the wave pumps to submerge during storm events; however there are no cost estimates for this design feature yet. The in-silico wave pump design currently is designed to be self-righting in all wave conditions, which helps to reduce storm damage. Third, the wave pumps would not experience significant degradation of performance over the twenty year lifetime, due to biofouling or otherwise. If these three assumptions regarding device deployment and performance are not substantiated, costs and resulting potential farm profit will be significantly affected.

Modifications to the design of the wave-powered water pump devices that increase the flow rate, while decreasing the cost of their manufacture will further enhance the kelp biomass yield and increase the feasibility of using wave pumps in kelp farms. These design considerations and wave pump improvements can continue to be investigated. The economic model based on a simple ROI lacks basic features of a typical cost model; however, with the present uncertainty in device cost, employing a more sophisticated economic model would be premature. While the transport and economic models are simple in nature, they indicate that wave pumps for kelp aquaculture may be economically feasible, and these models can be refined in future work.

Further work may include field studies which examine the impact of artificial upwelling on existing kelp farms. These efforts can validate the modeling efforts described within this article. Additionally, field studies present the opportunity to measure ecological effects from upwelling beyond temperature and nitrate changes, such as oxygen depletion, localized acidification, and harmful algal blooms via environmental monitoring. In geographical regions outside the Gulf of Maine, the case study would need to be repeated with applicable data sets to achieve relevant results (data sets would include: temperature, nitrate, wave conditions, irradiance, surface currents, kelp prices, etc.). Other methods to validate the one-dimensional transport model for nitrate and temperature could include three-dimensional, high-fidelity computational fluid dynamics (CFD) modeling or Regional Ocean Modeling System (ROMS). Several aspects relating to economic feasibility should be considered in further developing the wave pump concept. These include determining the fair market value for kelp in large-scale industry, and community endorsement of wave pumps by existing stakeholders. Socio-cultural integration of these devices in kelp mariculture likely depends upon proving and de-risking the technology, which can be accomplished with further laboratory and field validation experiments. While the US kelp mariculture industry does not currently operate at large scales (where wave pumps would be most practical), other global kelp mariculture industries may find these results useful at present. The US industry has the potential to expand kelp mariculture to larger scale, where the results of this work may be useful for increasing farm productivity.

Data availability statement

The raw data supporting the conclusions of this article will be made available by the authors, without undue reservation.

Author contributions

CK: Investigation, Writing – review & editing, Software, Writing – original draft, Validation, Conceptualization, Visualization, Methodology, Data curation, Formal analysis. MW: Funding acquisition, Supervision, Writing – review & editing, Resources, Conceptualization, Project administration, Methodology.

Funding

The author(s) declared that financial support was received for this work and/or its publication. This material is based upon work supported by the U.S. Department of Energy, Office of Science, Office of Critical Minerals and Energy Innovation, Hydropower and Hydrokinetic Office under Award Number DE-EE0009450.

Acknowledgments

The authors would like to thank Nathan Laxague and Tracy Mandel for their encouragement and support of this work. Additionally, discussions with Zach Moscicki and Kevin Hopkins have proven valuable in understanding potential benefits and challenges with artificial upwelling in kelp mariculture. Thank you to Teis Boderskov for sharing data on kelp biomass and corresponding available nitrate concentrations to draw comparisons to this work. Without the work done by Jim Irish and Dave

Fredriksson at the OOA and their valuable data set, this work would not be possible. The data set was provided by Rob Swift, who contributed many years of dedication to this project and provided the foundational knowledge for this work. The authors are perpetually grateful for his contributions and legacy. Many thanks to Chris Hunt for providing the uncertainty values for the nitrate measurements from the Jim Irish dataset. Thank you to the reviewers whose many constructive comments have helped to improve the quality of this article.

Conflict of interest

The author(s) declared that this work was conducted in the absence of any commercial or financial relationships that could be construed as a potential conflict of interest.

Generative AI statement

The author(s) declared that generative AI was not used in the creation of this manuscript.

Any alternative text (alt text) provided alongside figures in this article has been generated by Frontiers with the support of artificial intelligence and reasonable efforts have been made to ensure accuracy, including review by the authors wherever possible. If you identify any issues, please contact us.

Publisher's note

Supplementary material

The Supplementary Material for this article can be found online at: https://www.frontiersin.org/articles/10.3389/fmars.2026.1881744/full#supplementary-material

References

Augyte, S., Yarish, C., Redmond, S., and Kim, J. K. (2017). Cultivation of a morphologically distinct strain of the sugar kelp, Saccharina latissima forma angustissima, from coastal Maine, USA, with implications for ecosystem services. *J. Appl. Phycol.* 29 (4). doi: 10.1007/s10811-017-1102-x

B01 realtime doppler: Physical Oceanography Group, School of Marine Sciences, University of Maine. Northeastern Regional Association of Coastal Ocean Observing Systems. (2025). B01 realtime doppler current profile (ADCP) [Dataset].

Benitez-Nelson, C. R., Buesseler, K. O., and Crossin, G. (2000). Upper ocean carbon export, horizontal transport, and vertical eddy diffusivity in the southwestern gulf of maine. *Cont. Shelf Res.* 20, 707–736. doi: 10.1016/s0278-4343(99)00093-x

Boderskov, T., Rasmussen, M. B., and Bruhn, A. (2023). Upscaling cultivation of Saccharina latissima on net or line systems; comparing biomass yields and nutrient extraction potentials. *Front. Mar. Sci.* 10. doi: 10.3389/fmars.2023.992179

Bolton, J. J., and Luning, K. (1982). Optimal growth and maximal survival temperatures of Atlantic Laminaria species (phaeophyta) in culture. *Mar. Biol.* 66, 89–94. doi: 10.1007/bf00397259

Boufadel, M., Liu, R., Zhao, L., Lu, Y., Ozgökmen, T., Nedwed, T., et al. (2020). Transport of oil droplets in the upper ocean: impact of the eddy diffusivity. *J. Geophysical Res. Oceans.* 125 (2). doi: 10.1029/2019jc015727

Brenckman, C., Jayalakshmamma, M. P., Pennock, W., Ashraf, F., and Borgaonkar, A. D. (2025). A review of harmful algal blooms: causes, effects, monitoring, and prevention methods. *Water.* 17 (13), 1980. doi: 10.3390/w17131980

Broch, J., Omholt, A. M., Trine, B., Hege, G., Silje, F., Aleksander, H., et al. (2019). The kelp cultivation potential in coastal and offshore regions of Norway. *Front. Mar. Sci.* 5. doi: 10.3389/fmars.2018.00529

Broch, O., Ellingsen, I., Forbord, S., Wang, X., Volent, Z., and Alver, M. (2013). Modelling the cultivation and bioremediation potential of the kelp Saccharina latissima in close proximity to an exposed salmon farm in Norway. *Aquaculture Environ. Interact.* 4, 187–206. doi: 10.3354/aei00080

Broch, O., and Slagstad, D. (2012). Modelling seasonal growth and composition of the kelp Saccharina latissima. *J. Appl. Phycol.* 24, 759–776. doi: 10.1007/s10811-011-9695-y

Chambers, T. (2022). *A Comparative CO_2 Life Cycle Analysis of Three Nutrient Sources for a Novel Offshore Macroalgae Farm in Hawai'i* (Hilo, HI, USA: The University of Hawai'i at Hilo). Master's thesis.

Chereskin, T. K., and Harding, A. J. (1993). Modeling the performance of an acoustic doppler current profiler. *J. Atmos. Oceanic Technol.* 10, 41–63. doi: 10.1175/1520-0426(1993)010<0041:mtpoaa>2.0.co;2

Crowder, L. B., Ng, C. A., Frawley, T. H., Low, N. H., and Micheli, F. (2019). "The significance of ocean deoxygenation for kelp and other macroalgae," in *Ocean Deoxygenation: Everyone's Problem - Causes, Impacts, Consequences and Solutions*. Eds. D. Laffoley and J. M. Baxter (Gland, Switzerland: IUCN), 309–322. doi: 10.2305/IUCN.CH.2019.13.en

Davidson, P. A. (2015). *Turbulence: An Introduction for Scientists and Engineers* (Oxford, UK: Oxford University Press).

Department of Maine Resources. 2020-2024 Commercial Maine Landings (live pounds and value) by Species - table, PDF.

Department of Maine Resources (2015). Harvest of farm-raised marine algae in maine. 2015–20.

Dhakal, S., Juterbock, A. O., Lei, X., and Khanal, P. (2024). Application of the brown macroalga Saccharina latissima (Laminariales, Phaeophyceae) as a feed ingredient for livestock: a review. *Anim. Nutr.* 19, 153–165. doi: 10.1016/j.aninu.2024.07.001

Diehl, N., Steiner, N., Bischof, K., Karsten, U., and Heesch, S. (2023). Exploring intraspecific variability – biochemical and morphological traits of the sugar kelp Saccharina latissima along latitudinal and salinity gradients in europe. *Front. Mar. Sci.* 10. doi: 10.3389/fmars.2023.995982

Falnes, J. (2002). *Ocean Waves and Oscillating Systems* (Cambridge, UK: Cambridge University Press).

Fan, W., Chen, J., Pan, Y., Huang, H., Chen, C. T. A., and Chen, Y. (2013). Experimental study on the performance of an air-lift pump for artificial upwelling. *Ocean Eng.* 59, 47–57. doi: 10.1016/j.oceaneng.2012.11.014

FAO (2024). *Total Fisheries and Aquaculture Production: The State of the World Fisheries and Aquaculture 2024* (Rome, Italy: Food and Agriculture Organization of the United Nations). doi: 10.4060/cd0683en

Farghali, M., Mohamed, I., and Osman, A. (2023). Seaweed for climate mitigation, wastewater treatment, bioenergy, bioplastic, biochar, food, pharmaceuticals, and cosmetics: a review. *Environ. Chem. Lett.* 21, 97–152. doi: 10.1007/s10311-022-01520-y

Flavin, K., Flavin, B. F., and N., F. (2013). *Kelp Farming Manual: A Guide to the Processes, Techniques, and Equipment for Farming Kelp in New England Waters* (Saco, ME: Ocean Approved LLC).

Forbord, S., Etter, S., Broch, O., Dahlen, V., and Olsen, Y. (2021). Initial short-term nitrate uptake in juvenile, cultured Saccharina latissima (phaeophyceae) of variable nutritional state. *Aquat. Bot.* 168, 103306. doi: 10.1016/j.aquabot.2020.103306

Forbord, S., Mattson, S., Brodahl, G., Bluhm, B. A., and Broch, O. J. (2020). Latitudinal, seasonal and depth dependent variation in growth, chemical composition and biofouling of cultivated Saccharina latissima (Phaeophyceae) along the Norwegian coast. *J. Appl. Phycol.* doi: 10.1007/s10811-020-02038-y

Fredriksson, D. W., DeCew, J., Swift, M., Tsukrov, I., Chambers, M. D., and Celikkol, B. (2004). The design and analysis of a four-cage grid mooring for open ocean aquaculture. *Aquacult. Eng.* 32, 77–94. doi: 10.1016/j.aquaeng.2004.05.001

Freeman, D. S., and von Keitz, D. M. (2016). Macroalgae research inspiring novel energy resources. *Advanced Research Projects Agency - Energy. US Department of Energy*. 2016–26.

Gevaert, F., Davoult, D., Creach, A., Kling, R., Janquin, M. A., Seuront, L., et al. (2001). Carbon and nitrogen content of Laminaria saccharina in the eastern English Channel: biometrics and seasonal variations. *J. Mar. Biol. Assoc. U. K.* 81, 727–734. doi: 10.1017/S0025315401004532

GoogleEarth (2024). Coast of Maine, New Hampshire, Isles of Shoals.

Grebe, G. S., Byron, C. J., and et al, D. C. B. (2021). The nitrogen bioextraction potential of nearshore Saccharina latissima cultivation and harvest in the Western Gulf of Maine. *J. Appl. Phycol.* 33, 1741–1757. doi: 10.1007/s10811-021-02367-6

Grizzle, R., Ward, L., Langan, R., Schnaittacher, G., and Dijkstra, J. (2001). "Environmental monitoring in the vicinity of an open ocean aquaculture site in the southwestern gulf of maine: some preliminary results," in *Open Ocean Aquaculture IV Symposium Program and Abstracts*, (St. Andrews, NB, Canada: Fisheries and Oceans Canada), 58.

Hopkins, K. (2025). Personal communication. February 6th, 2025.

Hunt, C. (2026). *Personal communication. June 1st, 2026*.

Irish, J. (2010). Environmental data from the NH OOA site for aquaModel. Unpublished.

Karsten, U. (2007). Research note: salinity tolerance of arctic kelps from Spitsbergen. *Phycol. Res.* 55, 257–62. doi: 10.1111/j.1440-1835.2007.00468.x

Kilcher, L., Fogarty, M., and Lawson, M. (2021). Marine energy in the United States: an overview of opportunities. *Natl. Renewable Energy Lab*. doi: 10.2172/1766861

Kim, J. K., Kraemer, G. P., and Yarish, C. (2015). Use of sugar kelp aquaculture in Long Island Sound and the Bronx River Estuary for nutrient extraction. *Mar. Ecol. Prog. Ser*. 531, 155–166. doi: 10.3354/meps11331

Kimball, C., Swift, R., and Wosnik, M. (2025). Wave-powered water pump for upwelling in aquaculture: numerical model and ocean test. *Renewable Energy*. 239, 122040. doi: 10.1016/j.renene.2024.122040

Kimball, C., and Wosnik, M. (2025). "Wave-powered water pump design for improved performance", in: *Proceedings of the 16th European Wave and Tidal Energy Conference* (Madeira, Portugal), 16. doi: 10.36688/ewtec-2025-822

Kirke, B. (2003). Enhancing fish stocks with wave-powered artificial upwelling. *Ocean Coast. Manage.* 46, 901–915. doi: 10.1016/s0964-5691(03)00067-x

Kukulka, T., Proskurowski, G., Moret-Ferguson, S., Meyer, D. W., and Law, K. L. (2012). The effect of wind mixing on the vertical distribution of buoyant plastic debris. *Geophys. Res. Lett*. 39 (7). doi: 10.1029/2012gl051116

Lei, J., Fan, D., Angera, A., Liu, Y., and Nepf, H. (2021). Drag force and reconfiguration of cultivated Saccharina latissima in current. *Aquacult. Eng.* 94, 102169. doi: 10.1016/j.aquaeng.2021.102169

Levin, J. C., Grodsky, S. A., Vandemark, D., and Wilkin, J. L. (2022). Haline control of unusually deep winter mixing in the gulf of maine investigated using a regional data-assimilative model. *J. Geophysical Research: Oceans*. 127 (11). doi: 10.1002/essoar.10509004.1

Liu, Y., Cao, L., Cheung, W. W. L., and Sumaila, U. R. (2023). Global estimates of suitable areas for marine algae farming. *Environ. Res. Lett*. 18, 064028. doi: 10.1088/1748-9326/acd398

Liu, C. C. K., Dai, J. J., Lin, H., and Guo, F. (1999). Hydrodynamic performance of wave-driven artificial upwelling device. *J. Eng. Mech.* 125, 728–732. doi: 10.1061/(ASCE)0733-9399(1999)125:7(728)

Marine Energy Atlas: National Laboratory of the Rckies, US Department of Energy. Marine energy atlas.

McDowell Group (2018). "In brief mariculture development plan," (Alaska Mariculture Task Force).

Meuris, B., and Neary, V. (2024). "Characterization of wave energy resource and wave load conditions at atlantic marine energy center wave energy converter test sites," in *UMERC + METS 2024* (Duluth, MN, USA: University Marine Energy Research Conference + Marine Energy Technology Symposium), 17.

Min, B. R., Parker, D., Brauer, D., Waldrip, H., Lockard, C., Hales, K., et al. (2021). The role of seaweed as a potential dietary supplementation for enteric methane mitigation in ruminants: challenges and opportunities. *Anim. Nutr.* 7, 1371–1387. doi: 10.1016/j.aninu.2021.10.003

MODIS: NASA Goddard Space Flight Center, Ocean Ecology Laboratory, Ocean Biology Processing Group. (2014). MODIS-aqua ocean color data. doi: 10.1016/j.dsr2.2015.02.011

Molen, J., Ruardij, P., Mooney, K., Kerrison, P., O'Connor, N. E., and Gorman, E. (2018). Modelling potential production of macroalgae farms in UK and Dutch coastal waters. *Biogeosciences* 15, 1123–1147. doi: 10.5194/bg-15-1123-2018

Molina-Alcaide, E., Carro, M., Roleda, M., Weisbjerg, M., Lind, V., and Novoa-Garrido, M. (2017). *In vitro* ruminal fermentation and methane production of different seaweed species. *Anim. Feed Sci. Technol.* 228, 1–12. doi: 10.1016/j.anifeedsci.2017.03.012

Morel, A. (1988). Optical modeling of the upper ocean in relation to its biogenous matter content (case I waters). *J. Geophys. Res.* 93, 10749–10768. doi: 10.1029/JC093iC09p10749

Moscicki, Z. (2023). *Personal communication. May 18th, 2023*.

Moscicki, Z., Swift, M. R., Dewhurst, T., MacNicoll, M., Fredriksson, D. W., Chambers, M., et al. (2024). Evaluation of an experimental kelp farm's structural behavior using regression modelling and response amplitude operators derived from in situ measurements. *Ocean Eng.* 305, 117877. doi: 10.1097/01.lgt.0000383958.35852.33

Navarrete, I., Kim, D. Y., Wilcox, C., Reed, D. C., Ginsburg, D. W., Dutton, J. M., et al. (2021). Effects of depthcycling on nutrient uptake and biomass production in the giant kelp Macrocystis pyrifera. *Renewable Sustain. Energy Rev*. 141, 110747. doi: 10.1016/j.rser.2021.110747

NOAA National Data Buoy Center (1971). Meteorological and oceanographic data collected from the National Data Buoy Center Coastal-Marine Automated Network (C-MAN) and moored (weather) buoys. IOSN3 and 44030. (NOAA National Centers for Environmental Information). Available online at: https://www.ncei.noaa.gov/archive/accession/NDBC-CMANWx.

Patrick, A. (2014). Oscilla power's magnetostrictive wave energy generator successfully completes atlantic ocean tests.

Pawlowicz, R., and Yerubandi, R. (2024). *Wetzel's Limnology: Chapter 3 - Water as a Substance* (Oxford, UK: Academic Press), 15–24.

Pechsiri, J. S., Thomas, J. B. E., Risena, E., Ribeiroa, M. S., Malmstroma, M. E., Nylund, G. M., et al. (2016). Energy performance and greenhouse gas emissions of kelp cultivation for biogas and fertilizer recovery in Sweden. *Sci. Total Environ*. 573, 347–355. doi: 10.1016/j.scitotenv.2016.07.220

Pershing, A. J., Alexander, M. A., Brady, D. C., Brickman, D., Curchitser, E. N., Diamond, A. W., et al. (2021). Climate impacts on the gulf of maine ecosystem: a review of observed and expected changes in 2050 from rising temperatures. *Elementa: Sci. Anthropocene*. 9, 00076. doi: 10.1525/elementa.2020.00076

Peteiro, C., and Freire, O. (2012). Biomass yield and morphological features of the seaweed Saccharina latissima cultivated at two different sites in a coastal bay in the Atlantic coast of Spain. *J. Appl. Phycol.* 25, 205–213. doi: 10.1007/s10811-012-9854-9

Reid, G., Chopin, T., Robinson, S., Azevedo, P., Quniton, M., and Belyea, E. (2013). Weight ratios of the kelps, Alaria esculenta and Saccharina latissima, required to sequester dissolved inorganic nutrients and supply oxygen for Atlantic salmon, Salmo salar, in integrated multi-trophic aquaculture systems. *Aquaculture*. 408 and 409, 34–46. doi: 10.1016/j.aquaculture.2013.05.004

Robidoux, J., and Good, M. (2023). State of the states status of U.S. seaweed aquaculture. *Sea Grant Natl. Seaweed Symposium*.

Ruehl, K., Keester, A., Strofer, C. A. M., Tom, N., Topper, M., Lawson, M., et al. (2022). WEC-sim v5.0.1. doi: 10.5281/zenodo.10023797

Sanderson, J., Dring, M., Davidson, K., and Kelly, M. (2012). Culture, yield and bioremediation potential of Palmaria palmata (Linnaeus) Weber and Mohr and Saccharina latissima (Linnaeus) C.E. Lane, C.Mayes, Druehl and G.W. Saunders adjacent to fish farm cages in northwest Scotland. *Aquaculture*. 354, 128–135. doi: 10.1016/j.aquaculture.2012.03.019

Schakenbach, J. (2012). Neptune Wave Power, UNH partner on wave energy tech.

Schulz, K. G., Hartley, S., and Eyre, B. (2019). Upwelling amplifies ocean acidification on the east Australian shelf: implications for marine ecosystems. *Front. Mar. Sci*. 6. doi: 10.3389/fmars.2019.00636

Shan, S., and Sheng, J. (2022). Numerical study of topographic effects on wind-driven coastal upwelling on the scotian shelf. *J. Mar. Sci. Eng.* 10, 497. doi: 10.3390/jmse10040497

Sharma, S., Neves, L., Funderud, J., Mydland, L. T., Øverland, M., and Horn, S. J. (2018). Seasonal and depth variations in the chemical composition of cultivated Saccharina latissima. *Algal Res*. 32, 107–12. doi: 10.1016/j.algal.2018.03.012

Soloviev, A. V. (2016). "Ocean upwelling system utilizing energy of surface waves," in *2016 Techno-Ocean (Techno-Ocean)* (Kobe, Japan: IEEE), 221–224. doi: 10.1109/Techno-Ocean.2016.7890650

Strong-Wright, J., and Taylor, J. (2021). Modeling the growth potential of the kelp Saccharina latissima in the North Atlantic. *Front. Mar. Sci*. 8. doi: 10.3389/fmars.2021.793977

Sunniva, J. L., Silje, F., and Yngvar, O. (2020). The effect of nutrient availability and light conditions on the growth and intracellular nitrogen components of land-based cultivated Saccharina latissima (Phaeophyta). *Front. Mar. Sci*. 7. doi: 10.3389/fmars.2020.557460

Sylvers, L. H., Doall, M. H., Eckstein, M., Chen, L., and Gobler, C. (2025). Aquaculture of seaweeds (Saccharina latissima, Ulva spp., Gracilaria spp.) significantly improves the growth of co-cultivated bivalves in mesotrophic, but not eutrophic, estuaries. *Appl. Phycol.* 6, 398–417. doi: 10.1080/26388081.2025.2579943

Talley, L. D., Pickard, G. L., Emery, W. J., and Swift, J. H. (2011). *Descriptive Physical Oceanography an Introduction* (London, UK: Elsevier).

The MathWorks, Inc (2024). MATLAB version 24.2.0 (R2024b).

Townsend, D. W., and Larsen, P. F. (1992). *An Overview of Oceanography and Biological Productivity in the Gulf of Maine* (Washington D.C., USA: The Gulf of Maine–NOAA Coastal Ocean Program Regional Synthesis Series 1).

Townsend, D. W., Pettigrew, N. R., Thomas, M. A., and Moore, S. (2023). Warming waters of the gulf of maine: the role of shelf, slope and gulf stream water masses. *Prog. Oceanogr.* 215, 103030. doi: 10.1016/j.pocean.2023.103030

Tyrrell, H. J. V. (1964). The origin and present status of Fick's diffusion law. *J. Chem. Educ.* 41, 397–402. doi: 10.1021/ed041p397

V, G. S., M, D. K., Pugazhendi, A., Bajhaiya, A. K., Gugulothu, P., and J, R. B. (2021). Biofuel production from macroalgae: present scenario and future scope. *Bioengineered* 12, 9216–9238. doi: 10.1080/21655979.2021.1996019

Vaquer-Sunyer, R., and Duarte, C. M. (2008). Thresholds of hypoxia for marine biodiversity. *Proc. Natl. Acad. Sci.* 105, 15452–15457. doi: 10.1073/pnas.0803833105

Vershinskiy, N. V., Pshenichnyy, B. P., and Solov'yev, A. V. (1987). Artificial upwelling using the energy of surface waves. *Oceanology* 27, 400–402.

Vettori, D., and Nikora, V. (2017). Morphological and mechanical properties of blades of Saccharina latissima. *Estuar. Coast. Shelf Sci.* 196, 1–9. doi: 10.1016/j.ecss.2017.06.033

White, A., Bjorkman, K., Grabowski, E., Letelier, R., Poulos, S., Watkins, B., et al. (2010). An open ocean trial of controlled upwelling using wave pump technology. *J. Atmos. Oceanic Technol.* 27, 385–396. doi: 10.1175/2009jtecho679.1

Wilson, K. L., Kay, L. M., Schmidt, A. L., and Lotze, H. K. (2015). Effects of increasing water temperatures on survival and growth of ecologically and economically important seaweeds in atlantic Canada: implications for climate change. *Mar. Biol.* 162, 2431–2444. doi: 10.1007/s00227-015-2769-7

Zhang, L., Liao, W., Huang, Y., Wen, Y., Chu, Y., and Zhao, C. (2022). Global seaweed farming and processing in the past 20 years. *Food Prod. Process. Nutr.* 4, 23. doi: 10.1186/s43014-022-00103-2